Spinodal decomposition (phase transitions via unstable states)

V. P. Skripov and A. V. Skripov

Usp. Fiz. Nauk **128**, 193–231 (June 1979)

Considerable deviations from equilibrium conditions are observed for nonstatic, first-order phase transitions. In some cases, unstable (labile) phase states may precede the onset of the phase transition. The relaxation of the system is then accompanied by an enhancement of random inhomogeneities and the appearance of a modulated intermediate structure. This mechanism of the initial stage of a phase transition is called spinodal decomposition (SD). Theoretical and experimental studies of SD in two-component systems are reviewed in this paper. Thermodynamic stability and the possibility of SD in one-component liquid-vapor systems and an alternative nucleation mechanism are discussed. The phenomenological theory of SD is based on the Ginzburg-Landau expression for the free energy of an inhomogeneous system. A linearized diffusion equation is derived, for which thermodynamically unstable states have exponentially increasing solutions for the Fourier components of composition. Subsequent refinements of SD theory take into account thermal fluctuations and involve the derivation of the kinetic equation for the distribution functional. Diffraction methods are the most effective in the experimental study of SD in alloys, glasses, and binary liquid mixtures. So far, the agreement between theory and experiment must be regarded as only qualitative.

PACS numbers: 64.60. – i, 64.70.Fx, 64.80.Eb

CONTENTS

1. INTRODUCTION

The continuing interest in phase transitions has been due to their great variety and the unifying nature of the underlying physical principles. The rearrangement of super-molecular structures is accompanied by various manifestations of the fundamental properties of large ensembles of particles, revealing the underlying physical unity of phase transitions of different origin. For example, critical-type phase transitions are characterized by strong space-time correlation between particles, and a high level of fluctuations. This type of behavior signifies that the thermodynamic stability boundary, i. e., the spinodal, is being approached. The spinodal bounds the region of unstable (labile) homogeneous states and touches the phase coexistence curve at the critical point.

When the phase transition process is fast, one (or both) of the coexisting phases lies outside the region of completely stable states. Studies of nonequilibrium phase transitions and, in particular, of transition kinetics, are currently very topical and of considerable practical imporatnce (in connection with the intensification of heat and mass transfer, the production of ultrafine grains or supercooled amprohous alloys, and so on).

Spinodal decomposition (SD) is a special case of the initial stage of a phase transformation in which the system is first made to be in a labile state $[(\partial\mu/\partial n)_{T,p}<0]$. The relaxation of the system is then accompanied by the enhancement of random inhomogeneities in the particle distribution, and the appearance of modulated relaxation structures is found to be possible.

Metallurgists were the first to draw attention to the unusual mechanism of phase separation, and introduced the concept of uphill diffusion ($D<0$). Phenomena in certain glasses were then identified as belonging to this type of transformation. Spinodal decomposition is currently being studied in stratified solutions of polymers and in ordinary binary liquid solutions having a region of limited miscibility.

The first publications on the phenomenological theory of spinodal decomposition appeared in the early 1960's.[1,2] They described a general linearized diffusion equation for a two-component system and a solution of this equation that contained an amplification factor in time that was increasing for unstable states. Prior to this (in 1940), the physical conditions underlying SD in one-component systems were examined by Zel'dovich and Todes.[3]

There has been considerable progress in experimental

 0038-5670/79/060389-22$01.10

and theoretical studies of SD in the course of the last decade. The phenomenon itself is of considerable interest in physics generally, but is still not familiar enough to a broad circle of physicists. The aim of the present review is to present the basic ideas and current research into spinodal decomposition. The connection between SD and the usual mechanism of phase transitions of the first kind is also discussed, including activated nucleation and the growth of the coexisting new phase.

2. TWO TYPES OF PHASE STABILITY. UPHILL DIFFUSION

For a long time, studies of phase transitions were confined to the quasistatic approximation. The phenomenological description of heterogeneous systems developed by Gibbs[4] and the advent of statistical interpretations of thermodynamics[5] provided a satisfactory theoretical basis for the study of phase equilibria and the corresponding phase transitions. The next stage in the development of studies of phase transitions relied to a considerable extent on Gibbs' results in the field of surface phenomena and the stability of phase states. By taking surface free energy (surface tension σ) into account, it was possible to describe systems containing a dispersed phase. Gibbs obtained an expression for the work done W_* in producing a critical nucleus in terms of measurable macroscopic quantities. Volmer and Weber[6] then proposed the following expression for the time-independent frequency J of spontaneous nucleation per unit volume:

$$J = N_1 B e^{-W_*/k_B T}, \tag{2.1}$$

where N_1 is the number of molecules of the initial phase per unit volume and B is a kinetic factor to be determined. The form of this factor was subsequently established[7-12] and it was shown that the preexponential expression $N_1 B$ was a slowly varying function of temperature and pressure. An increase in J to an appreciable value requires a sharp reduction in W_* when the homogeneous system becomes supersaturated as it goes into the region of metastable states.

The dimensionless parameter $G = W_*/k_B T$ characterizes the relative height of the free-energy barrier during nucleation. The chances of overcoming this barrier as a result of thermal fluctuations increase with decreasing G, so that this parameter may be looked upon as a measure of the stability of the system against discontinuous changes of a known kind (appearance of a new phase). In the case of a plane separation boundary, the equilibrium phase coexistence curve corresponds to $G \to \infty$. This curve defines the absolute stability boundary for the competing phases, and regions of metastable states (with finite G) are adjacent to it. We may take $G = 0$ as the lower limit of stability of this type.

A more important property for our ensuing discussion will be the stability of a phase against continuous changes of state corresponding to small perturbations of density (concentration) and energy in macroscopic portions of the system. A state is stable if the corresponding phase has a restoring reaction, so that the perturbation is resorbed by the system. In the case of unstable states, small perturbations grow as a result of the response of the system. Metastable states are assumed to be stable against continuous changes and are adjacent to the region of absolute instability during high supersaturation.

In the case of fast processes, it is important to take into account not only metastable but also labile states of a homogeneous system.

Nonstatic processes are characterized by the ratios of several characteristic times. For example, to estimate the depth of penetration of the metastable region, we must know the characteristic time $\mathcal{T}$ of the experiment, the mean expectation time $\langle\tau\rangle$ of a nucleus in a volume element ΔV, and the phase decomposition time τ_p for this element in the presence of the nucleus. The quantities $\langle\tau\rangle$ and τ_p depend on the degree of supersaturation, and the inquality $\mathcal{T}/(\langle\tau\rangle+\tau_p) \ll 1$ signifies the absence of any significant indication of a phase transition in a system kept in the metastable state for a time of the order of τ. Maximum supersaturation corresponds to

$$\frac{\mathcal{T}}{\langle\tau\rangle+\tau_p} \approx 1. \tag{2.2}$$

Systems are often found to contain the seeds of a phase transition, i. e., so-called active centers. The volume density Ω of the number of such centers increases with increasing degree of supersaturation. It is convenient to take $\Delta V = \Omega^{-1}$, so that (2.2) is an implicit function of Ω. Unfortunately, very little is known about Ω. It depends on the method of preparation of the system, the properties of the walls, and the properties of impurity solid particles. The case of a "pure" system ($\Omega = 0$) is better defined physically. The mean time $\langle\tau\rangle$ can then be estimated from the Volmer-Döring-Zel'dovich-Frenkel' (FDZF) theory; see Chap. 7. In most cases, the phase separation time τ_p is estimated from the corresponding thermal or diffusion problem. We note that phase transitions initiated by fluctuational nuclei can also appear in the presence of active centers if the metastable state is penetrated rapidly enough.[1)] This situation can occur, for example, in bubble chambers.

The time τ_p increases rapidly near the critical point of two-phase equilibrium. The region of metastable states is then found to contract to a point. These two facts provide a favorable foundation for reaching unstable states with the aid of a near-critical transition through the binodal and the spinodal.

Figure 1 shows the diagram of state for a one-component liquid-vapor system ($v = 1/\rho$ is the specific volume, T is the temperature, and K is the critical point). The binodal (1) corresponds to the situation where the chemical potentials of the liquid and vapor are equal temperatures and pressures of the coexisting phases:

$$\mu'(p, T) = \mu''(p, T).$$

The spinodal (2) separates the regions of positive and

[1)] There are no kinetic difficulties, as in the case of vitrified liquids.

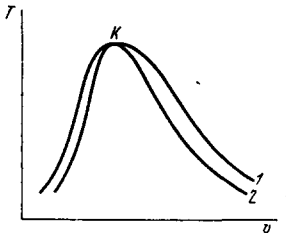

FIG. 1. Binodal (1) and spinodal (2) curves for a one-component liquid-vapor system (*K* is the critical point).

negative values of these drivatives $(\partial p/\partial \rho)_T, (\partial T/\partial S)_p$. These derivatives vanish on the spinodal. This means that the thermodynamic response functions, namely, the isothermal compressibility β_T and the isobaric specific heat C_p will diverge. In addition, the condition $(\partial p/\partial \rho)_T = 0$ also means that $(\partial \mu/\partial \rho)_T = 0$ or $(\partial \mu/\partial n)_T = 0$ because, in the case of the one-component system, we have

$$\left(\frac{\partial p}{\partial \rho}\right)_T = \rho \left(\frac{\partial \mu}{\partial \rho}\right)_T,$$

where $\rho = mn$ and m is the mass of a molecule.

The adiabatic derivative $(\partial p/\partial \rho)_S$ evidently remains positive as we cross the spinodal.

In the labile state $[(\partial p/\partial \rho)_T < 0]$, a medium will rapidly lose spatial homogeneity and will relax by assuming a cellular-grainy structure without phase boundaries. The usual heterogeneity in which one of the coexisting phases is dispersed in the presence of a stable surface layer sets in at a later stage. Spinodal decomposition is understood to mean the development of continuously inhomogeneous structure as a result of thermodynamic instability.

The kinetics of this kind of process in a one-component system was first examined by Zel'dovich and Todes.[3] So long as the medium is stable against adiabatic perturbations, the rate of spinodal decomposition is limited by heat transfer between contracting and expanding volume elements. The coefficient of temperature diffusivity $\alpha = \lambda/\rho C_p$ and the specific heat at constant pressure C_p become negative as we cross the spinodal. This is equivalent to time reversal in the thermal conductivity equation

$$\frac{\partial T}{\partial t} = \alpha \Delta T.$$

In the simplest case, this results in solutions with exponentially growing local temperature differences appearing against a background of an increase in the spatial inhomogeneity in the density of the medium. Temperature equalization occurs when the volume elements leave the region of labile states. The characteristic SD time is given by the following order-of-magnitude expression:

$$\tau_c = \frac{l^2}{|\alpha|}.$$

The lower limit of the characteristic linear size l has been estimated[3] as being of the order of the effective thickness of the equilibrium surface (interphase) layer at a given temperature. The corresponding analysis was performed near the critical point where τ_c is expected to be not too small because of the asymptotic divergence of C_p and l $(C_p \to \infty, \alpha \to 0, l \to \infty)$. The following approximate expression was obtained for water:[3]

$$\tau_c = \frac{2 \cdot 10^{-6}}{(T_c - T)^2} \text{ (sec)}.$$

The time of "preparation" of the unstable state necessary for the observation of SD must be less than τ_c.

Two-component (multicomponent) systems are also found to have a region of unstable homogeneous states. This may take the form of stratification of liquid or solid solutions with a critical temperature of equilibrium coexistence of condensed phases, or systems with a liquid-vapor critical point. Deviation from stability sets in as a result of local deviations from equilibrium composition. If a random inhomogeneity in composition is not resorbed into the system but, instead, is amplified by the response of the system, the situation corresponds to a negative diffusion coefficient D (uphill diffusion). For two-component systems, the onset of diffusion instability precedes mechanical instability.[13] Figure 2 shows the phase diagram at atmospheric pressure for the binary system consisting of isobutyric acid and water[14] with an upper critical temperature of solution. When $T < T_c$, the liquid phases that coexist in equilibrium have relative concentrations lying on the binodal AKB on which the chemical potentials μ of each of the phase components are equal.

The condition for diffusion stability is $(T, p = \text{const})$

$$\frac{\partial \mu_1}{\partial x_1} > 0, \tag{2.3}$$

where x_1 is the molar fraction of the first component.

A similar inequality is satisfied for the second component. The Gibbs-Duhem relation

$$x_1 \, d\mu_1 + x_2 \, d\mu_2 = 0, \qquad T, \; p = \text{const}$$

and the condition $x_1 + x_2 = 1$ lead to the following relation between the derivatives of the chemical potential:

$$\frac{\partial \mu_2}{\partial x_2} = \frac{x_1}{x_2} \frac{\partial \mu_1}{\partial x_1}. \tag{2.4}$$

For unstable states under the dome aKb, we have $(\partial \mu_1/\partial x_1) < 0$. The spinodal corresponds to the limit of diffusion stability and is defined by

$$\frac{\partial \mu_1}{\partial x_1} = 0. \tag{2.5}$$

It is occasionally more convenient to use not the chem-

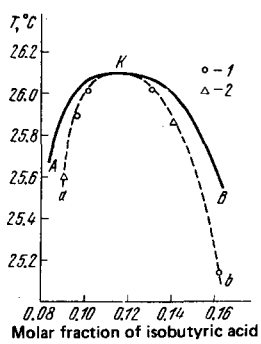

FIG. 2. Phase diagram for the system consisting of isobutyric acid and water:[14] *AKB* is the binodal curve and *aKb* the spinodal curve. The latter is drawn through the experimental points obtained by extrapolating light scattering data (1) and Rayleigh linewidths (2).

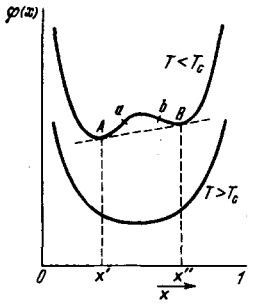

FIG. 3. Molar thermodynamic Gibbs potential as a function of concentration in a two-component stratified solution at temperatures below and above the critical point.

ical potentials but the molar Gibbs potential

$$\varphi = x_1\mu_1 + x_2\mu_2. \tag{2.6}$$

It is readily shown that

$$\frac{\partial\varphi}{\partial x_1}=\mu_1-\mu_2, \qquad \frac{\partial^2\varphi}{\partial x_1^2}=\frac{1}{x_2}\frac{\partial\mu_1}{\partial x_1}. \tag{2.7}$$

When $x_1, x_2 \neq 0$, the derivative $\partial\mu_1/\partial x_1$ in (2.3) and (2.5) can be replaced with the derivative $\partial^2\varphi/\partial x_1^2$.

Figure 3 shows a schematic plot of the molar potential φ as a function of concentration for two temperatures, one below and one above the critical point. This plot was constructed on the assumption that $\varphi(x)$ was continuous and analytic. The lower curve ($T > T_c$) is always convex to the composition axis. This ensures diffusion stability of the solution throughout the range of concentrations, $\partial^2\varphi/\partial x_1^2 > 0$, and, at the same time, ensures that the system cannot separate into coexisting phases.[2)] The upper curve has both convex and concave segments. The turning points a, b belong to the boundary of stability of homogeneous states and $\partial^2\varphi/\partial x_1^2 = 0$. The points A, B on the common tangent to the convex segments of the curve correspond to coexisting condensed phases in equilibrium.

We now turn to the equation for isothermal diffusion in a two-component condensed system. In the approximation of linear thermodynamics of irreversible processes, the diffusion motive force is the gradient of the chemical potential. If we consider the molecular currents j_1 and j_2 of the components relative to the surface on which $j_1 + j_2 = 0$ the equation for the current assumes the form

$$j_1 = -L(\nabla\mu_1 - \nabla\mu_2); \tag{2.8}$$

where L is the Onsager coefficient ($L_{11} = L_{22} = -L_{12} = L > 0$), which characterizes the mobility of the molecules. If we write the chemical potential gradient in terms of the concentration gradient and use (2.4), we obtain

$$j_1 = -L\frac{\partial\mu_1}{\partial x_1}\frac{1}{x_2}\nabla x_1 = -Dn\nabla x_1; \tag{2.9}$$

where

$$D = \frac{L}{n}\frac{1}{x_2}\frac{\partial\mu_1}{\partial x_1} = \frac{L}{n}\frac{\partial^2\varphi}{\partial x_1^2}, \tag{2.10}$$

and $n = n_1 + n_2$ is the number of molecules per unit volume.

It is clear from the foregoing expressions that there is a connection between mass transport and the parameter of thermodynamic stability $\partial\mu_1/\partial x_1$ or $\partial^2\varphi/\partial x_1^2$. The mutual diffusion coefficient is proportional to this parameter. As the stability boundary is approached, $D \to 0$. A considerable slowing down of the diffusion transport is, in fact, observed near the critical point of two-component liquid systems.[15] For unstable states, we have $D < 0$, i. e., uphill diffusion in the direction of the concentration gradient.

The behavior of the mobility L near the stability boundary is not clear from the phenomenological analysis. This is still a matter of dispute in the literature. The expressions given by (2.9) and (2.10) are hardly suitable for a quantitative description of transport phenomena near the spinodal. A modified linearized diffusion equation which takes into account the fluctuation inhomogeneity of the system will be considered below.

When phase transitions in solutions and their stability are discussed, one can use either the thermodynamic Gibbs potential Φ, φ, or the free energy F, f. Since, for a two-component system consisting of $N_1 + N_2$ molecules we have

$$F = \Phi - pV = \mu_1 N_1 + \mu_2 N_2 - pV,$$
$$f = \frac{F}{N_1 + N_2} = \varphi - pv = \mu_1 x_1 + \mu_2 x_2 - pv,$$

the replacement of φ by f in expressions containing only increments and derivatives of these quantities is legitimate provided the increment on the last term (pv) is small. For condensed systems, this approximation can be used in (2.7) and (2.10) with $\partial\varphi/\partial x_1, \partial^2\varphi/\partial x^2$ replaced by $\partial f/\partial x_1, \partial^2 f/\partial x_1^2$. Finally, we note one further point in relation to molar and volume (per unit volume) values of μ, φ, and f. Transformation to volume quantities leads to the appearance of factors containing molecular masses of the components and the concentrations in formulas such as (2.9). We shall use the same notation for both molar and volume quantities, and will not write out the transformation factors.

When the state of a system undergoes a rapid change, the thermodynamic degrees of freedom do not succeed in reaching the state of complete equilibrium. It is reasonable to suppose that the relaxation time t_1 of degrees of freedom corresponding to lengths $l_1 > l_c$ (l_c is the correlation length) is much greater than the relaxation time t_2 of degrees of freedom corresponding to scales $l_2 \ll l_1$. This assumption is justified by the fact that the instability of the system is connected with long-wave fluctuations, whilst short-wave fluctuations remain stable (see Chap. 3). It follows that, in a time $t_2 \ll t_1$, local equilibrium is established in small regions $l_2 \ll l_1$, so that we can introduce local thermodynamic variables. The theory of spinodal decomposition describes the relaxation of these variables over times $t > t_2$. We note that the validity of this assumption improves near the spinodal, where the scales l_1 and t_1 are large. In most cases, however, one uses the additional assumption that the relaxation time of one hydrodynamic mode (for example, concentration) is much greater than the relaxation time of all the other parameters of the system.

[2)]We are ignoring the vapor phase.

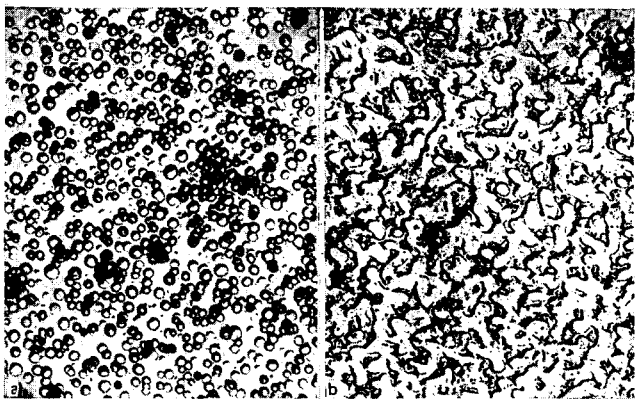

FIG. 4. Electron-microscope photographs of two-phase glasses:[22] a—structure obtained from metastable state through nucleation and growth; b—structure ascribed to spinodal decomposition.

Let us now briefly consider the experimental material that has led to the development of current ideas on spinodal decomposition. Of major importance has been the discovery of a periodic distribution of separating phases (modulated structure) during the decomposition of a solid solution into two phases whidh differ only in concentration and lattice parameters. This modulated structure was first observed by Daniel and Lipson[16,17] in the Cu–Ni–Fe alloy. They found that the principal x-ray reflections corresponding to the single-phase structure were accompanied by satellites. These satellites can be explained by assuming that the lattic parameter and the Cu concentration vary periodically in the direction of the crystallographic axes. The period of this modulated structure is of the order of 100 Å. The modulated structures have now been observed directly with the electron microscope (see, for example, Refs. 18–20). A detailed analysis of such structures in different solid solutions has been reported by Khachaturyan.[21] Phase separation (liquation) in glasses is also accompanied by the appearance of a composition-inhomogeneous structure, and the phase separation exhibits a kind of periodicity. This type of liquation structure is illustrated in Fig. 4. A large number of examples of observed liquation structures and glasses can be found in the literature.[23,24]

The appearance of uphill diffusion was first discussed in connection with experimental data on the ageing of Cu–Al alloys,[25] and was then examined theoretically[26,27]. The development of ideas on spinodal decomposition is reviewed by Cahn[28] and Chuistov.[29]

3. PHENOMENOLOGICAL THEORY OF SPINODAL DECOMPOSITION

We shall now review the phenomenological theory of spinodal decomposition developed by Cahn and Hilliard,[30] Hillert,[1] and Cahn.[2,31-33] The free energy of a two-component isotropic solution can be written in the form

$$F = \int [f(x) + K(\nabla x)^2]\, dV, \tag{3.1}$$

where $f(x)$ is the free-energy density[3)] of the homogeneous solution of composition x and $K(\nabla x)^2$ is the first nonvanishing term of the expansion of $f[x(\mathbf{r})]$ in a Taylor series in $\mathbf{r}$. It describes the contribution of space-correlated effects to free energy. Cutting off the expansion at the second-order term is equivalent to the assumption that the range of the intermolecular potentials is much smaller than the characteristic lengths over which there is an appreciable change in the concentration. It is also assumed that the molar volume is independent of composition. $K>0$ if the homogeneous state is stable above the spinodal. In general, K can depend on concentration.

If the concentration at each point in the solution is not very different from the mean concentration x_0, the expansion of $f(x)$ in terms of $x-x_0$ need not be continued beyond the quadratic term. If, in addition, we recall that

$$\int (x - x_0)\, dV = 0$$

we find that the free-energy difference between the solution with concentration fluctuations and the completely uniform solution of concentration x_0 is

$$\Delta F = F - f(x_0)V = \int \left[\frac{1}{2}\frac{\partial^2 f}{\partial x_0^2}(x-x_0)^2 + K(\nabla x)^2\right] dV.$$

The Fourier representation is convenient for the analysis of the stability of a solution against infinitesimal changes in composition. If we expand $x-x_0$ in Fourier series

$$x - x_0 = \sum_{\mathbf{k}} A(\mathbf{k})\, e^{i\mathbf{k}\mathbf{r}},$$

we obtain

$$\Delta F = \frac{1}{2} V \sum_{\mathbf{k}} |A(\mathbf{k})|^2 \left(\frac{\partial^2 f}{\partial x_0^2} + 2Kk^2\right).$$

The solution is stable against infinitesimal changes in concentration if $\partial^2 f/\partial x_0^2 + 2Kk^2 > 0$ for all k. Since $K>0$, this condition is always satisfied for states with $\partial^2 f/\partial x_0^2 > 0$ (the temperature exceeds the spinodal temperature). In the interior of the spinodal, i.e., in the region where $\partial^2 f/\partial x_0^2 < 0$, the quantity $\partial^2 f/\partial x_0^2 + 2Kk^2$ is negative if $k < k_c$, where

$$k_c = \sqrt{-\frac{1}{2K}\frac{\partial^2 f}{\partial x_0^2}}. \tag{3.2}$$

The solution is, therefore, unstable in the interior of the spinodal against infinitesimal fluctuations in concentration with wavelengths $\lambda > \lambda_c = 2\pi/k_c$.

The kinetics of spinodal decomposition can be obtained by solving the diffusion equation given by (2.8). The difference between the chemical potentials is expressed in terms of the functional derivative $\delta F\{x(\mathbf{r})\}/\delta x(\mathbf{r})$:

$$\mu_1 - \mu_2 = \frac{1}{V}\frac{\delta F}{\delta x_1},$$

and $\delta F/\partial x_1$ is calculated from (3.1). We have

$$\mathbf{j}_1 = -L\nabla\left[\frac{\partial f}{\partial x_1} - 2K\nabla^2 x_1 - \frac{\partial K}{\partial x_1}(\nabla x_1)^2\right]. \tag{3.3}$$

Neglecting the dependence of K on concentration, taking

[3)] It is assumed that $f(x)$ can also be defined in the region where the two-phase state is stable; in this case, we must look upon $f(x)$ as the analytic continuation of the free-energy density of the homogeneous system into the two-phase region.

the divergence of both sides of (3.3), and using the equation of continuity, we obtain

$$\frac{\partial x}{\partial t} = L\nabla^2\left(\frac{\partial f}{\partial x} - 2K\nabla^2 x\right). \tag{3.4}$$

During the early stages of decomposition, the concentration fluctuations are small and only terms that are linear in x need be retained on the right-hand side of (3.4). This yields the linearized diffusion equation

$$\frac{\partial x}{\partial t} = L\left(\frac{\partial^2 f}{\partial x_0^2}\nabla^2 x - 2K\nabla^4 x\right). \tag{3.5}$$

We now write the solution of this equation as a Fourier series

$$x(\mathbf{r}, t) - x_0 = \sum_{\mathbf{k}} A(\mathbf{k}, t) e^{i\mathbf{kr}}, \tag{3.6}$$

where

$$A(\mathbf{k}, t) = A(\mathbf{k}, 0)\, e^{R(\mathbf{k})t}, \tag{3.7}$$

$$R(\mathbf{k}) = -Lk^2\left(\frac{\partial^2 f}{\partial x_0^2} + 2Kk^2\right). \tag{3.8}$$

The function $R(k)$ is called the amplification factor. Its dependence on wave number is shown schematically in Fig. 5. It is negative for all k in the metastable region ($\partial^2 d/\partial x_0^2 > 0$) and positive for $k < k_c$ in the region of unstable states ($\partial^2 f/\partial x_0^2 < 0$). The critical wave number k_c is given by (3.2). Consequently, in the labile range of concentrations, waves with $k < k_c$ will grow exponentially, whereas those with $k > k_c$ will decay exponentially. Waves with wave number $k_m = k_c/\sqrt{2}$ will grow most rapidly. Since $R(k)$ is present in the argument of the exponential in (3.7), and the dependence of the amplification factor on wave number has a relatively sharp maximum at $k = k_m$, we assume that all the concentration waves other than those corresponding to k_m can be neglected after a certain interval of time. As a result, the system develops a characteristic length scale $\lambda_m = 2\pi/k_m$ and the composition of the isotropic solution in this approximation can be described as a superposition of sinusoidal waves of fixed wavelength λ_m and random orientations, phases, and amplitudes.

The theory of spinodal decomposition based on the linearized diffusion equation given by (3.5) is valid only during the initial stages of decomposition when the deviations of composition from the mean are small. It predicts an unbounded growth in concentration fluctuations. If the deviations of concentration from the mean cease to be small, the diffusion equation can no longer be confined to terms that are linear in x. Inclusion of the higher-order terms in x leads to a distortion of the shape of the sinusoidal concentration waves and to a restriction of their growth.[34] Khachaturyan[21] has pointed out that a situation is possible where the nonlinear terms become important even prior to the emergence of the characteristic size λ_m in the system. This is expected near the spinodal.

FIG. 5. Amplification factor as a function of wave number.

We have assumed so far that the molar volume is independent of concentration. When this is not so, concentration fluctuations in a solid can be accompanied by elastic stresses contributing to the total free energy of the system. This energy can then be written in the form

$$F = \int [f(x) + K(\nabla x)^2 + \eta^2 Y (x - x_0)^2]\, dV,$$

where η is the relative change in the lattice parameter a accompanying the change in composition:

$$\eta = \frac{1}{a}\frac{da}{dx},$$

and Y is a parameter that can be defined in terms of the elastic constants ($Y > 0$). The elastic energy stabilizes the solid solution against small fluctuations in concentration, and the condition for loss of stability now becomes:

$$\frac{\partial^2 f}{\partial x_0^2} + 2\eta^2 Y = 0; \tag{3.9}$$

where $f(x)$ is the free-energy density in the absence of stresses. This condition defines (within the framework of the linear approximation to the theory of spinodal decomposition) the so-called "coherent" spinodal which is shifted toward lower temperatures from the "chemical" spinodal defined by $\partial^2 d/\partial x_0^2 = 0$. For some alloys, this shift amounts to some hundreds of degrees.

In the case of elastically anisotropic solid solutions, Y depends on the crystallographic direction in the material. Loss of stability occurs first for concentration waves with orientations corresponding to minimum Y. The modulated structure that appears as a result of the decomposition process is thus found to be "attached" to definite crystallographic axes.

When elastic energy is taken into account in the linearized diffusion equation (3.5) and in the expressions given by (3.2) and (3.8), the second derivative $\partial^2 f/\partial x_0^2$ must be replaced with $\partial^2 f/\partial x_0^2 + 2\eta^2 Y$. The term associated with elastic energy will be omitted from now on.

The theory of spinodal composition given by Cahn has been generalized to the case of ternary systems[35] and to decomposition during continuous cooling.[36]

The experimentally observed quantity is usuall the scattered x-ray intensity $I(\mathbf{s}, t)$, where $\mathbf{s}$ is the scattered wave vector, $|\mathbf{s}| = 4\pi \sin(\theta/2)/\Lambda$, Λ is the wavelength of the radiation, and θ is the angle between the incident and scattered rays. In the Born approximation,

$$I(\mathbf{s}, t) \sim |A(\mathbf{k}, t)|^2 \text{ for } \mathbf{k} = \mathbf{s}. \tag{3.10}$$

The intensity $I(\mathbf{s}, t)$ can thus yield direct information on the spectrum of composition fluctuations in the system. The expression (3.10) was first used by Rundman and Hilliard[37] in the analysis of small-angle x-ray scattering data, obtained for a decomposing Al-Zn alloy.

Since the time evolution of $A(\mathbf{k}, t)$ is determined by (3.7) within the framework of the linearized theory of spinodal decomposition, we may write

$$I(\mathbf{k}, t) = I(\mathbf{k}, 0)\, e^{2R(\mathbf{k})t}. \tag{3.11}$$

Consequently, Cahn's theory predicts an exponential increase in I for $k < k_c$ and an exponential decay for k

$> k_c$ in the labile region. For $k = k_c$, the scattered intensity should be time-independent; this is the point of intersection of the $I(\mathbf{k})$ curves corresponding to different t. The expression given by (3.11) can be used as a basis for the experimental verification of the spinodal decomposition theory. The amplification factor can be found from the best correspondence between experimental data and (3.11). Additional verification of the theory involves checking the dependence of R on wave number. According to (3.8), the graph of $R(k)/k^2$ vs k^2 should be a straight line.

4. DEVELOPMENT OF THE THEORY

A serious defect of the theory of spinodal decomposition put forward by Cahn was that it did not take into account thermal fluctuations in composition. The theory does not, therefore, contain mechanisms responsible for transitions from unstable to stable configurations, and leads to incorrect equilibrium behavior of the scattered intensity $I(\mathbf{k}, t)$. In fact, for stable states $R(k) < 0$, and, according to (3.11), any initial distribution $I(\mathbf{k}, 0)$ should fall to zero. On the other hand, it is well known that experiment shows that $I(\mathbf{k}, \infty)$ is not zero and is associated with fluctuation inhomogeneities. Cook[38] has extended diffusion equation (2.8) by adding a term responsible for the fluctuation thermal contribution to the current $\mathbf{j}$. The equation for $I(\mathbf{k}, t)$ thus becomes

$$\frac{\partial I(\mathbf{k}, t)}{\partial t} = 2R(\mathbf{k}) I(\mathbf{k}, t) + 2Lk_B T k^2. \tag{4.1}$$

Its solution is

$$I(\mathbf{k}, t) = [I(\mathbf{k}, 0) - I(\mathbf{k}, \infty)] e^{2R(k)t} + I(\mathbf{k}, \infty), \tag{4.2}$$

where

$$I(\mathbf{k}, \infty) = \frac{k_B T}{(\partial^2 f/\partial x_0^2) + 2Kk^2} = \frac{k_B T}{2K(k^2 - k_c^2)}. \tag{4.3}$$

Appreciable deviations from the behavior predicted by Cahn's theory are observed when the condition $I(\mathbf{k}, 0) \gg I(\mathbf{k}, \infty)$ is not satisfied. It follows from (4.2) that the growth of the Fourier components of concentration occurs not only for $R(k) > 0$ but also for $R(k) < 0$ if $I(\mathbf{k}, 0) < I(\mathbf{k}, \infty)$. Cook's theory is thus seen to predict a shift of the observed critical wave vector from the value k_c given by (3.2). According to (4.1), the observed critical wave vector k_c' at $t = 0$ is determined by the condition

$$\left(\frac{\partial^2 f}{\partial x_0^2} + 2Kk^2\right) I(\mathbf{k}, 0) - k_B T = 0,$$

i. e., $k_c' > k_c$. Cook's theory provides a qualitative explanation of the deviation from Cahn's theory that has been demonstrated by many experiments (Chap. 5), namely, the deviation from the exponential variation of $I(\mathbf{k}, t)$ especially for $k > k_c$, the curvature of the graph of $(\partial I/\partial t)/Ik^2$ as a function of k^2, and the fact that the critical wave number is much greater than $\sqrt{2}k_m$, where k_m is the wave number corresponding to maximum growth.

However, Cook's theory again predicts an unbounded growth of Fourier components of composition for $k < k_c$ in the region of unstable states. As noted by Langer,[40,41] it does not yield the correct expression for the equilibrium scattered intensity at temperatures below the stratification temperature. In fact, at the end of phase separation, when the system has assumed the equilibrium configuration, one would expect $I(\mathbf{k}, \infty)$ to follow the well-known Ornstein-Zernike formula

$$I(\mathbf{k}, \infty) \sim \frac{k_B T}{2K(k^2 + \gamma^2)}, \tag{4.4}$$

where γ is the reciprocal correlation length. Comparison of (4.4) with (4.3) will show that, in (4.3), γ is an imaginary quantity. This contradiction arises because the derivative $\partial^2 f/\partial x^2$ is evaluated at $x = x_0$ in (4.3) and is always negative at temperatures below the stratification temperature. On the other hand, the correct approach at the end of the phase separation stage is to expand f around the equilibrium phase compositions. The second derivative $\partial^2 f/\partial x^2$ is then positive for each phase.

Langer[39-42] has developed a more rigorous theory of spinodal decomposition based on the statistical approach to the problem. He began by constructing the equation of motion not for the function $x(\mathbf{r}, t)$ but for the statistical distribution $\rho(\{x\}, t)$ over configurations $x(\mathbf{r})$. The transport equation then has the form of a functional continuity equation[39]

$$\frac{\partial \rho[\{x\}, t)}{\partial t} = -\int \frac{\delta J(\mathbf{r})}{\delta x(\mathbf{r})} d\mathbf{r}, \tag{4.5}$$

where

$$J(\mathbf{r}) = L\nabla^2 \left(\frac{\delta F}{\delta x(\mathbf{r})} \rho + k_B T \frac{\delta \rho}{\delta x(\mathbf{r})}\right). \tag{4.6}$$

The average of any functional $V\{x\}$ is then defined in the usual way

$$\langle V(t)\rangle = \sum_{\{x\}} \rho(\{x\}, t) V\{x\}, \tag{4.7}$$

where the sum goes over all long-wave variations in composition consistent with the mean composition x_0. Equations (4.5), (4.6), and (4.7) then lead Langer to the following equation of motion:

$$\frac{\partial \langle x\rangle}{\partial t} = L\nabla^2 \left(\left\langle \frac{\partial f}{\partial x} \right\rangle - 2K\nabla^2 \langle x\rangle\right). \tag{4.8}$$

Expanding $\partial f/\partial x$ in series in the neighborhood of x_0 and retaining only first-order terms, we obtain the linearized diffusion equation (3.5). This, however, does not mean that (4.8) is equivalent to the generalized nonlinear diffusion equation of Cahn, given by (3.4), because $\langle \partial f/\partial x\rangle$ is not identical with $\partial f(\langle x\rangle)/\partial \langle x\rangle$ provided only ρ does not have a very sharp maximum near some configuration $x(\mathbf{r})$. The assumption that the distribution of ρ has zero width is equivalent to neglecting fluctuations in the nonlinear diffusion equation of Cahn. In the Langer approach, fluctuations are taken into account automatically through the finite width of the distribution ρ.

The structure factor $S(\mathbf{k}, t)$, which is proportional to the scattered intensity $I(\mathbf{k}, t)$, is particularly interesting. This factor is related to the correlation function for concentration fluctuations $G(\mathbf{r}, t)$ through the Fourier transformation

$$S(\mathbf{k}, t) = \int G(\mathbf{r}, t) e^{i\mathbf{k}\mathbf{r}} d\mathbf{r}, \tag{4.9}$$

where

$$G(\mathbf{r}, t) = G(|\mathbf{r}|, t) = \langle u(\mathbf{r}_0 + \mathbf{r}, t) u(\mathbf{r}_0, t)\rangle, \qquad u(\mathbf{r}, t) = x(\mathbf{r}, t) - x_0. \tag{4.10}$$

If we use (4.9), (4.10) together with the transport equation (4.5), we can write the equation of motion for $S(\mathbf{k}, t)$ in the form[42]

$$\frac{\partial S(\mathbf{k}, t)}{\partial t} = -2Lk^2\left[\left(\frac{\partial^2 f}{\partial x_0^2} + 2Kk^2\right) S(\mathbf{k}, t) + \frac{1}{2}\frac{\partial^3 f}{\partial x_0^3} S_3(\mathbf{k}, t) + \frac{1}{6}\frac{\partial^4 f}{\partial x_0^4} S_4(\mathbf{k}, t) + \ldots\right] + 2Lk_B T k^2, \tag{4.11}$$

where $S_n(\mathbf{k}, t)$ are the Fourier transforms of the correlation functions $G_n(\mathbf{r}, t)$ of order n:

$$G_n(\mathbf{r}, t) = \langle u^{n-1}(\mathbf{r}_0 + \mathbf{r}, t)\, u(\mathbf{r}_0, t)\rangle \tag{4.12}$$

(we shall omit the subscript $n=2$ on S and G). The series in (4.11) appears as a result of the expansion of $\langle \partial f/\partial x\rangle$ in Taylor series. If we retain only the term that is linear in x in this expression, we obtain

$$\frac{\partial S(\mathbf{k}, t)}{\partial t} = 2R(\mathbf{k}) S(\mathbf{k}, t) + 2Lk_B T k^2, \tag{4.13}$$

which is identical with Cook's result, given by (4.1). The next approximation could be referred to as the mean-field approximation. It is obtained from (4.11) by assuming that $\rho\{x\}$ is always a Gaussian distribution over the functions $u(\mathbf{r})$, centered on $u \equiv 0$. This approximation is satisfactory so long as the most probable value $u(\mathbf{r})$ is zero and the fluctuations are relatively small. When this is so, $G_n = 0$ for all odd n and

$$S_4(\mathbf{k}, t) \approx 3\langle u^2(t)\rangle S(\mathbf{k}, t),$$

where, according to (4.9) and (4.10),

$$\langle u^2(t)\rangle = \frac{1}{(2\pi)^3}\int S(\mathbf{k}, t)\, d\mathbf{k}. \tag{4.14}$$

If in the expansion for $\langle \partial f/\partial x\rangle$ we retain only terms up to third order in x, we obtain

$$\frac{\partial S(\mathbf{k}, t)}{\partial t} = 2\tilde{R}(\mathbf{k}, t) S(\mathbf{k}, t) + 2Lk_B T k^2, \tag{4.15}$$

where

$$\tilde{R}(\mathbf{k}, t) = -Lk^2\left(\frac{\partial^2 f}{\partial x_0^2} + \frac{1}{2}\frac{\partial^4 f}{\partial x_0^4}\langle u^2(t)\rangle + 2Kk^2\right). \tag{4.16}$$

Since $\langle u^2(t)\rangle$ is a positive function that increases with time in the case of spinodal decomposition, $\tilde{R}$ will decrease in the case of positive $\partial^4 f/\partial x_0^4$, and this will lead to a restriction of the growth of the unstable Fourier components of concentration. On the other hand, the critical wave number will decrease with time, which gives a qualitatively correct description of the increase in the characteristic scale (coarseness) in the system. However, the mean-field approximation suffers from serious defects that prevent its use in the description of subsequent stages of spinodal decomposition. Thus, firstly, fluctuation in $u(\mathbf{r})$ should not be expected to be small and centered on $u \equiv 0$ during the decomposition process. It is clear that, during the later stages, the distribution ρ will have maxima near values of u for which $x_0 + u$ is an equilibrium concentration. Secondly, the mean-field approximation does not take into account the asymmetry of fluctuations (the term proportional to $\partial^3 f/\partial x_0^3$ is neglected), which may be important near the spinodal. Thirdly, numerical analyses[42] have shown that the quantity $[(\partial^2 f/\partial x_0^2) + 1/2(\partial^4 f/\partial x_0^4)\langle u^2(t)\rangle]/2K$, which here plays the role of γ^2 in (4.4), does not change sign in the course of time and remains negative. The mean-field approximation does not, therefore, provide the correct expression for the equilibrium intensity below the stratification temperature.

Langer developed two methods to overcome the limitations of the mean-field approximation. The first[40] is based on the expansion of $u(\mathbf{r})$ over the complete set of orthonormal basis functions $\psi_{lm}(r)$, introduced by Wilson,[43]

$$u(\mathbf{r}) = \sum_{lm} a_{lm}\psi_{lm}(\mathbf{r}),$$

where $\psi_{lm}(r)$ is the basis function localized near a definite site R_m, the Fourier components of which lie inside the l-th spherical shell in k-space:

$$\frac{k_{\max}}{2^{l+1}} < k < \frac{k_{\max}}{2^l}$$

($k_{\max}$ is the radius of the Wigner-Seitz sphere). The existence of this set of basis functions is merely a hypothesis, and the explicit form of these functions is not known. However, important results can be obtained without knowing the explicit form of ψ_{lm}. By introducing certain further assumptions, we can rewrite the transport equation and obtain an equation of motion for functions of $u(\mathbf{r})$ in the language of the new variables a_{lm}. The functions in which we are interested, for example, $S(\mathbf{k}, t)$, are estimated only for a discrete set of values of the wave number, which is a consequence of the subdivision of reciprocal space into spherical layers and the fact that we do not know the explicit form of ψ_{lm}. We shall not reproduce here the rather unwieldy equations of motion for $I(k_l, t)$ and turn immediately to the results of their numerical solution.[41] The input parameters for the numerical solution were taken from the papers of de Fontaine[44] and Rundman and Hilliard.[37] The results are shown in Fig. 6 together with the corresponding results based on Cook's theory[38] and the mean-field approximation [Eqs. (4.15), (4.16), and (4.14)]. It is clear from Fig. 6 that graphs of $\ln I(k_l, t)$ as a function of l have no appreciable linear segments. In contrast to previous theories of spinodal decomposition, Langer's method yields a qualitatively correct solution in the limit of long times. It is also clear from Fig. 6 that a characteristic size emerges in the system: the $l=4$ mode has a much greater amplitude than all the other modes. Moreover, in this approach, the quantity $[\partial^2 f/\partial x_0^2) + 1/2(\partial^4 f/\partial x_0^4)\langle u^2(t)\rangle]/2K$ changes sign in the course of time, and approaches a positive equilibrium value, thus ensuring the correct form (4.4) for $I(\mathbf{k}, \infty)$.

The other approach, resulting in an approximate solution of (4.11), is based on the assumption of some rea-

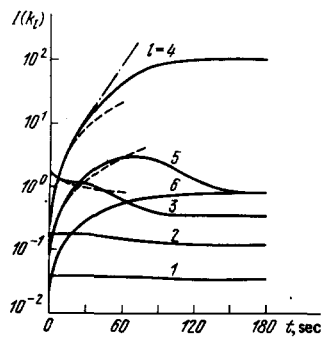

FIG. 6. Numerical solution of the equations of motion:[41] $k_1 = 6.22\times10^7$ cm^{-1}, $k_2 = 3.11\times10^7$ cm^{-1}, $k_3 = 1.56\times10^7$ cm^{-1}, $k_4 = 0.778\times10^7$ cm^{-1}, $k_5 = 0.389\times10^7$ cm^{-1}, $k_6 = 0.194\times10^7$ cm^{-1}. The dot-dash curve is predicted by Cook for $l=4$; the dashed curves are calculated in the mean field approximation for $l=3$, 4, and 5.

sonable form[42] for the distribution ρ. It follows from (4.12) that, to determine the right-hand side of (4.11), it is sufficient to know the two-point distribution function $\rho_2[u(\mathbf{r}_0+\mathbf{r}), u(\mathbf{r}_0)]$. This is obtained by integrating the complete distribution $\rho\{u\}$ over the space of functions u, the values of which are fixed at the two points $\mathbf{r}_0+\mathbf{r}$ and $\mathbf{r}_0$. It is assumed that the relation between ρ_2 and the one-point functions ρ_1 is

$$\rho_2[u(\mathbf{r}_0+\mathbf{r}), u(\mathbf{r}_0)] \approx \rho_1[u(\mathbf{r}_0+\mathbf{r})]\,\rho_1[u(\mathbf{r}_0)]\{1+\gamma(\mathbf{r})\,u(\mathbf{r}_0+\mathbf{r})\,u(\mathbf{r}_0)\}.$$

This assumption is equivalent to keeping the first two terms in the expansion of ρ_2 in terms of the functions $u(\mathbf{r}_0+\mathbf{r})$ and $u(\mathbf{r}_0)$. In this approximation,

$$G(\mathbf{r}) = \langle u^2\rangle^2\,\gamma(\mathbf{r})$$

and

$$G_n(\mathbf{r}) \approx \frac{\langle u^n\rangle}{\langle u^2\rangle} G(\mathbf{r}).$$

Equation (4.11) assumes the form

$$\frac{\partial S(\mathbf{k}, t)}{\partial t} = -2Lk^2[2Kk^2 + C(t)]\,S(\mathbf{k}, t) + 2Lk_BTk^2, \tag{4.17}$$

where

$$C = \sum_{n=2}^{\infty} \frac{1}{(n-1)!}\frac{\partial^n f}{\partial x_0^n}\frac{\langle u^n\rangle}{\langle u^2\rangle} = \frac{1}{\langle u^2\rangle}\left\langle u\frac{\partial f(x_0+u)}{\partial u}\right\rangle.$$

Since C is a one-point function, it is determined if we know ρ_1. The sum of two shifted Gaussian functions is a physically reasonable form for ρ_1:

$$\rho_1(u) = \frac{a_1}{\sqrt{2\pi}\,\sigma}\exp\left[-\frac{(u-b_1)^2}{2\sigma^2}\right] + \frac{a_2}{\sqrt{2\pi}\,\sigma}\exp\left[-\frac{(u+b_2)^2}{2\sigma^2}\right].$$

This function enables us to describe both the early stages of spinodal decomposition when ρ_1 is centered on $u=0$ ($b_1, b_2 \ll \sigma$), and the subsequent stages when ρ_1 has two maxima ($b_1+b_2>\sigma$), in the language of variations in $a_1, a_2, b_1, b_2, \sigma$. Because of the normalization conditions

$$\int \rho_1(u)\,du = 1$$

and

$$\int \rho_1(u)\,u\,du = 0$$

only three of these five parameters are independent. The independent parameters are found from the equations of motion for $\langle u^2\rangle$, $\langle u^3\rangle$, and $\langle u^4\rangle$, which are derived from the transport equation for ρ_1. The transport equation for ρ_1, in turn, can be obtained from the transport equation (4.5) for the complete distribution $\rho\{u\}$.[42] Numerical calculation based on this scheme[42] yields a qualitatively correct description of the decomposition process: the growth of the maximum of $S(\mathbf{k}, t)$ and its shift in the course of time toward smaller k, the appearance of two maxima in the distribution function $\rho_1(u)$, and the growth of the separation between these maxima. The time dependence of $S(\mathbf{k}, t)$ is not always exponential, as predicted by Cahn's linearized theory, and the graph of $[\partial S(k,t)/\partial t]/S(k,t)k^2$ as a function of k^2 is appreciably nonlinear for all t.

An approach based on the transport equation for the distribution ρ was also used in[45]. In contrast to the other treatment,[42] the representation in the form of a sum of shifted Gaussian functions was used not for the one-point distribution function for ρ_1 but for the complete functional $\rho[\{A(\mathbf{k})\}, t]$, in reciprocal space. The theory given in Ref. 45 (like the Langer theory) takes fluctuations into account in a natural way and can be used to describe both the early and the late stages of spinodal decomposition.

The theory of the early stages of spinodal decomposition in a liquid near the critical point was recently developed independently by Kawasaki.[46-48] The transport equation (3.5) was modified by adding a nonlocal term describing the hydrodynamic interaction between fluctuations in the order parameter. The inclusion of hydrodynamic effects enabled Kawasaki to improve the agreement between theory and experiment in binary liquid mixtures.[47] However, the Kawasaki formulation contains a number of assumptions that are difficult to control.

Patashinskiĭ and Yakub[49] have put forward a simple phenomenological approach demonstrating the similarity properties of the relaxation of systems with conserved order parameter in the region of unstable states. They have also examined decomposition during cooling at a finite rate, and a theory of the initial stage of spinodal decomposition in a one-component liquid-vapor system.[50] Simultaneous solution of the Navier-Stokes equation, the continuity equation, and the equation of state leads to a growth in the long-wave fluctuations in density and temperature in the labile region.

We note that all the above approaches are based on the use of (3.1) for the free energy of the inhomogeneous solution. It is clear, however, that this equation is not rigorous. Free energy can be expressed[51,52] in terms of the two-body interaction potentials, the radial particle distribution functions, and the local concentration $x(\mathbf{r})$ in the form of double space integrals. If we expand $x(\mathbf{r})$ in a Taylor series in the integrand, and retain only the first nonvanishing term, we obtain (3.1), where

$$K = \frac{\pi}{3}\int_0^{\infty} \Omega(r)\,r^4\,dr, \tag{4.18}$$

$$\Omega(r) = g_A(\varphi_{AB}-\varphi_{AA}) + g_B(\varphi_{AB}-\varphi_{BB}),$$

g_i are the radial distribution functions for atoms of type i, and φ_{ij} is the two-body interaction potential between atoms of types i and j. If the interaction potential has a large enough range, higher order terms must be included in the expansion for $x(\mathbf{r})$. However, Hopper and Uhlmann[52] have shown that, for typical potentials, the coefficients of $\nabla^{2n}x$ diverge, beginning with $n=2$. To avoid a nonphysical result, $x(\mathbf{r})$ can be expanded into a Fourier rather than a Taylor series.[52] This leads to an exact expression for F. The diffusion equation is subsequently introduced in the same way as in Cahn's theory. In particular, the Fourier components of the concentration are found to vary exponentially during the early stage of the decomposition process. The amplification factor, however, is different from (3.8):

$$R'(k) = Lk^2\left[-\frac{\partial^2 f}{\partial x_0^2} - 2B(k)\right],$$

$$B(k) = 2\pi\int_0^{\infty}\left(1-\frac{1}{kr}\sin kr\right)r^2\Omega(r)\,dr.$$

If the integral in (4.18) converges (short-range interaction), the function $B(k)$ tends to Kk^2 in the limit of small k. $B(k)$ is appreciably different from Kk^2 for large val-

ues of k, and the graph of $R'(k)/k^2$ as a function of k^2 is not linear. For potentials that decrease with distance more slowly than r^{-5}, the function $B(k)$ is not quadratic in k even for small k.[53] The Hopper-Uhlmann theory is thus capable of quantitative estimation of the amplification factor if the interaction potentials are known. However, as in Cahn's theory, it is, in fact, assumed in the derivation of the expression for F that there is no short-range order in the system.[52] For systems with developed fluctuations, neither (3.1) not the Hopper-Uhlmann results for F appear to be exact.

Abraham[54,55] has constructed a thermodynamic description of an inhomogeneous one-component liquid system, based on a generalization of perturbation theory to liquids.[56,57] His results for the free energy and the amplification factor are equivalent to the corresponding results given by Hopper and Uhlmann. The determinations of φ and g, reported in Refs. 56 and 57, were employed. Abraham's theory can also be generalized to the case of two-component liquid mixtures.[58] The Hopper-Uhlmann and Abraham approaches derive the decomposition kinetics from the microscopic theory, but they still suffer from all the defects that attend the neglect of fluctuations.

A new formulation of the theory of spinodal decomposition in the language of the Ising model with conserved order parameter has recently been put forward by Binder.[59] Each lattice site is assigned a "spin" value $X_i=+1$ if it is occupied by an atom of type A, and $X_i=-1$ if it is occupied by an atom of type B. In this model, relaxation occurs through the exchange of neighboring atoms. The Hamiltonian for the system has the well-known form

$$\mathcal{H} = -\sum_{j\neq i} J_{ij}X_iX_j - \sum_i H_iX_i + \mathcal{H}_0,$$

where J_{ij}, H_i, and $\mathcal{H}_0$ can be expressed in terms of the two-body interaction potentials φ_{AA}, φ_{BB}, and φ_{AB}. The transport equation[60] for the probability $P(X_1,\ldots,X_N,t)$ of realization of the "spin" configuration $(X_1,\ldots,X_N)$ at time t is then written down and used to obtain an equation of motion for the mean of any function $\langle X_1,\ldots,X_N\rangle$, in particular for $S(\mathbf{k},t)$, the Fourier transform of the spatial two-body correlation function $\langle X_i(t)X_j(t)\rangle - \langle X_i(t)\rangle \times\langle X_j(t)\rangle$. In this approach, the equation of motion for $S(\mathbf{k},t)$ is exact but not closed, since it contains higher-order correlation functions. Additional simplifying assumptions are necessary to close it. Under certain assumptions,[59] the exact equation yields approximate equations of motion for $S(\mathbf{k},t)$ that are equivalent to the corresponding equations in the Cahn, Cook (4.13), and Langer (4.17) theories. The earlier results can thus be derived from the Ising model, i. e., through an approach that is radically different from the original approach. To proceed further, Binder[59] proposed an abbreviated description in the language of cluster distribution. The transport equation for the cluster concentration $\bar{n}_l(t)$ is derived from the transport equation for $P(X_1,\ldots,X_N,t)$, where l is the number of atoms per cluster and the bar represents averaging over the coordinates of the "centers of gravity" of all the clusters. The cluster model is convenient for the description of late stages of decomposition, examined qualitatively in Ref. 61. Numerical calculations based on the cluster model[62] yield the following law for the growth of the mean linear size of a grain during late stages of phase decomposition, examined qualitatively in Ref. 61. Numerical calculations based on the cluster model[62] yield the following law for the growth of the mean linear size of a grain during late stages of phase decomposition: $\bar{R}\sim t^b$, where the exponent is less than 1/3 (the value predicted by Lifshitz and Slezov[63]). Calculations[62] have also shown that the cluster size distribution is very broad. The Binder approach suffers from a number of defects. The most important is that lattice distortions accompanying phase separation and the associated elastic stresses cannot be taken into account.

5. EXPERIMENT

A. Alloys

Historically, the first class of systems in which spinodal decomposition was investigated experimentally was that involving two- and three-component alloys. There is now a large number of publications on phase separation in alloys in the immiscible region. However, it is by no means always possible to obtain an unambiguous identification of the mechanism responsible for phase separation. The final morphology of alloys undergoing spinodal decomposition cannot always be distinguished from that corresponding to nucleation and growth. In particular, modulated structure may appear as a result of nucleation and growth,[18] so that structure periodicity is not a reliable criterion for spinodal decomposition. Neither this method nor electron microscopy are very useful for the identification of the phase separation mechanism, although analysis of the isothermal sequence of microstructures does often lead to quite reliable conclusions.[64-66]

The usual thermal treatment of alloys in experiments concerned with phase-separation kinetics is as follows. The specimen is homogenized by annealing at high temperature (in the single-phase region) and is then rapidly quenched down to room temperature. It is assumed that no appreciable phase separation occurs during the quenching process. The alloy is then held at the temperature at which decomposition is observed (in the immiscible region) for a time t, and is again quenched. As a rule, measurements are performed at room temperature. By varying t, one can obtain information on the phase-separation kinetics.

Since the theory of spinodal decomposition is formulated in reciprocal space, diffraction methods (primarily, x-ray diffraction) provide the most direct verification of this theory. The original studies of phase-decomposition kinetics were performed by a method based on the observation of satellite of principal Bragg reflections.[16] The position of the satellites was used to determine the wavelength λ_m of the modulated structure and its variation during decomposition. It is clear that this method can, at best, reveal only a qualitative agreement with the concept of spinodal decomposition, namely, the fact the λ_m remains constant during the early stages and increases during the coarsening stage. This behavior has been observed, for example, in an Au-Pt alloy.[67]

Rundman and Hilliard[37] used small-angle x-ray scattering to investigate the phase separation kinetics in Al-22 at .% Zn. Their analysis of experimental data was based on (3.10). It follows from

$$\frac{4\pi}{\Lambda}\sin\frac{\theta}{2}=|\mathbf{s}|=|\mathbf{k}|=\frac{2\pi}{\lambda}$$

that, when composition fluctuations with wavelength $\lambda \approx 40$Å are observed for $\Lambda \approx 4$Å, the necessary scattering angles are $\theta \approx 1.5°$. The scattered x-ray intensity is directly related to the spectrum of concentration fluctuations in the system, which enabled Rundman and Hilliard to perform a quantitative comparison between experiment and the theory of spinodal decomposition. They found good agreement with Cahn's theory when the temperature was held at 65 °C and, in particular, they found that $I(\mathbf{k}, t)$ varied exponentially with time over a period of several minutes [in agreement with (3.11)] and that the graph of $R(k)/k^2$ against k^2 was nearly linear [as in (3.8)]. However, Gerold and Merz[68] used measurements of the integrated scattered x-ray intensity for the same system to conclude that Rundman and Hilliard[37] observed a coarsening of the structure, and that spinodal decomposition was already nearly complete during the quenching stage. The integrated scattered intensity[69]

$$\mathcal{J}=\int I(k)\,k^2dk\sim\int (x-x_0)^2\,dV$$

can be used to characterize the degree of completion of phase separation. It is expected that $\mathcal{J}$ will initially increase rapidly and then remain constant when the equilibrium compositions are reached. Gerold and Merz[68] observed the following behavior of $\mathcal{J}$ for the Al-22 at .% Zn alloy: at the very beginning of the isothermal process, when the specimen was held at 65 °C, the integrated intensity $\mathcal{J}$ was found to increase sharply, and this could be explained by a change in the equilibrium phase composition at this temperature as compared with room temperature; thereafter, $\mathcal{J}$ remained constant. The conclusion[68] that decomposition is almost complete during the quenching of the Al-22 at .% Zn system has also been confirmed elsewhere.[70,71] The agreement with Cahn's theory reported in Ref. 37 would therefore appear to have been fortuitous.

Agarwal and Herman[72] quenched their specimens from the melt as a means of observing the early stages of decomposition in the Al-22 at .% Zn alloy. Figure 7 shows their data on small-angle x-ray scattering for different types of heat treatment at 65 °C. For the specimen that was not subjected to the heat treatment ($t=0$), the intensity I was practically independent of k, indicating that the quenching was sufficiently rapid. When the specimen was held under isothermal conditions, the $I(k)$ curve had a peak whose amplitude increased with time and whose position shifted slowly toward smaller k. The observation of a common point of intersection of the $I(k)$ curves suggests that k_c was constant. The intensity $I(k,t)$ varied roughly exponentially for all the k that were investigated up to ~50 min. The dependence of $R(k)/k^2$ on k^2 was, however, highly nonlinear. Unfortunately, Agarwal and Herman[72] do not report any data on the integrated scattered intensity that might have yielded some information on the degree of completion

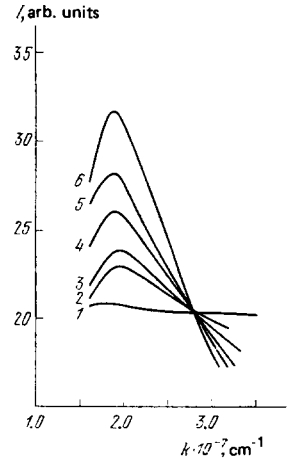

FIG. 7. Small-angle x-ray scattering intensity for Al-22% Zn.[22] Heat treatment time at 65 °C (sec): 0 (1), 45 (2), 90 (3), 180 (4), 300 (5), and 1200 (6).

of the decomposition process at different times.

Spinodal decomposition has been established quite reliably[73,74] in Al-Zn alloys with a lower concentration of zinc (in particular, Al-6.8 at .% Zn). Small-angle scattered x-ray intensities were used[73] to determine the interval during which decomposition was effective for different heat treatment temperatures (Fig. 8). The intensity $I(k,t)$ was a nearly exponential function of t during this interval.

If the alloy consists of atoms in neighboring positions in the periodic table, x-ray and electron diffraction turn out to be ineffective as a means of investigating phase separation. This is so because the scattering factors are then too close together, and neutron scattering must be employed. Small-angle neutron scattering has been used, for example, to investigate spinodal decomposition in Fe-Cr, Cu-Ni, and Al-Zn (Refs. 75, 76, and 77, 78, respectively).

In addition to diffraction methods, phase separation

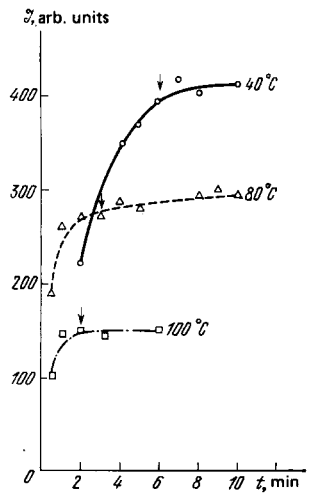

FIG. 8. Integrated x-ray scattering intensity as a function of time of heat treatment at 40, 80, and 100 °C for Al-6.8 at .% Zn.[73] Arrows mark the time interval of effective decomposition.

kinetics in the immiscible region has also been investigated by measuring resistivity[79] and magnetic susceptibility,[80] and by studying nuclear magnetic resonance[81,82] and the Mössbauer effect.[83,84] In particular, the Mössbauer effect can be used very successfully to distinguish between nucleation and growth mechanisms, on the one hand, and spinodal decomposition, on the other hand, in the Fe-Cr system.[83,84] This is so because one of the equilibrium phases (chromium-enriched) is paramagnetic at the working temperature, whereas the other and the mean composition of the alloy are ferromagnetic at this temperature. The paramagnetic peak should, therefore, appear in the nuclear gamma-resonance method right from the beginning of the thermal-treatment process if there is nucleation. On the other hand, during spinodal decomposition, one should observe only a broadening of the line corresponding to the quenched alloy, and the paramagnetic peak should appear only at the end of the decomposition process. Both phase separation mechanisms were observed, depending on the composition and the temperature of heat treatment.

Both ordering and decomposition are possible in some alloys. A detailed study of the Fe–Al system with these properties has been carried out by Allen and Cahn.[85] The Fe–Al phase diagram has a tricritical point at which the continuous-ordering line intersects the binodal curve bounding the immiscible region. Depending on composition and heat treatment conditions, different sequences of different types of phase transformation and a large number of final morphologies are observed in this alloy. Allen and Cahn[85] used a thermodynamic analysis to formulate general rules for establishing the order in which different types of phase transition follow one another. In particular, they showed that metastable continuations of continuous-ordering lines into the immiscible region were effectively the spinodal curves in the sense that they bounded the region in which phase separation of composition components was possible but only if preliminary ordering had taken place. Electron microscopy data[85] are in qualitative agreement with these predictions on the sequence of phase transformation mechanisms. Ordering and decomposition are also observed in Cu–Be (Ref. 86), Cu–Ti (Ref. 65), and Ni–Ti (Refs. 66,87). In Cu–Be, ordering precedes spinodal decomposition whereas, in Cu–Ti and Ni–Ti, spinodal decomposition precedes ordering. According to Allen and Cahn,[85] one cannot exclude the possibility of a change in the sequence of mechanisms in these systems as the alloy concentration and heat treatment conditions are varied.

It is important to note that, despite the large number of publications in which the idea of spinodal decomposition is used to interpret experimental results, there is a lack of papers devoted to the quantitative verification of the spinodal decomposition theory. Measurements of mutual diffusion coefficients in Au–Ag (Ref. 88) and Cu–Pd (Ref. 89) are very valuable from this point of view. The diffusion coefficients have been determined from the rate of relaxation of composition modulation produced artificially by layered deposition of components from the vapor phase. These measurements have been interpreted[88,89] as demonstrating the validity of the modified Cahn diffusion equation (34) in the description of homogenization kinetics in these alloys.

B. Glasses

Glasses have turned out to be relatively convenient systems for verifying the idea of spinodal decomposition. The high viscosity of glasses, and their low diffusion coefficients in the immiscible region, impede phase separation, so that early stages of the process can be observed. Moreover, elastic stresses or anisotropy, which usually complicate the decomposition picture, are commonly absent.

The identification of the phase separation mechanism is usually the basic problem that arises in the experimental study of phase-separation kinetics. First attempts to detect spinodal decomposition of glasses involved observations of the morphology of liquating glasses. Cahn[33] showed that the two-phase structure that appeared during spinodal decomposition should be characterized by a high degree of phase coherence. This type of structure can be seen during the phase separation occurring in many glasses (Fig. 4b) and was for some time regarded as a criterion for spinodal decomposition.[90] However, it was subsequently demonstrated[91] that this highly cohesive structure could also appear as a result of nucleation and growth. This conclusion was confirmed by Seward *et al.*,[92] who used electron microscopy to investigate phase separation in the $BaO–SiO_2$ system. During the early stages, they observed isolated and almost spherical particles that are characteristic of nucleation, and this was followed by formation of a highly cohesive two-phase structure. Consequently, as in the case of metal alloys, the morphology of liquating glasses could not be used as a criterion for the onset of spinodal decomposition.

More profound information on phase-separation kinetics can be obtained by diffraction methods, namely, small-angle x-ray scattering and light scattering. Experimental results have usually been compared with the linearized Cahn theory, i.e., a check was made on (3.11) for the dependence of $(\partial I/\partial t)/Ik^2$ on k^2. Most of the measurements were concerned with $Na_2O–SiO_2$[93-95] and $Ba_2O_3–PbO–Al_2O_3$.[96-98] The specimens were rapidly quenched from the single-phase region and then held at constant temperature in the range 350–600 °C. The scattered intensity was measured as a function of the angle of scattering and the time of heat treatment. The overall character of the family of curves representing $I(k,t)$ is the same as for metal alloys (Fig. 7). Most publications report that the dependence of I on time was nearly exponential. However, there were several cases[98-99] in which deviations were noted from the exponential form during the very early stages of the decomposition process. Craievich[98] has reported that these deviations may have been due to structural relaxation in rapidly quenched glasses.

The most important discrepancies as compared with Cahn's theory have been found in the case of the amplification factor R as a function of wave number. According to Cahn's theory, R/k^2 should be a linear function of

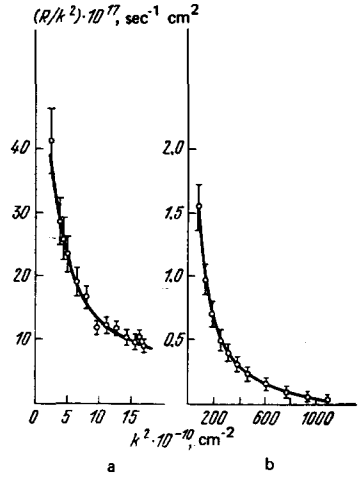

FIG. 9. R/k^2 plotted against k^2 for SiO_2–12.5% Na_2O glass at 530 °C according to light scattering (a) and small-angle x-ray scattering (b) data.[95]

k^2, whereas all experimental evidence shows that there are considerable deviations from the linear relation, especially for small k. As an example, Fig. 9 shows the results of Andreev *et al.*,[35] showing the highly nonlinear behavior of R/k^2 as a function of k^2 over a broad range of values of k. Moreover, in most publications, a common point of intersection of $I(k)$ curves corresponding to different t was not observed in the early stages. Still more surprising is the fact that a common point of intersection occasionally appears during the late stages of decomposition when the linear Cahn theory is no longer valid.[99] This result was explained by Srinivasan *et al.*[97] If terms beyond the quadratic term in the expansion of $f(x)$ are neglected, a rapid transfer of the system to the region under the spinodal curve corresponds to $I(k,0)<I(k,t)$ for all k. According to Cook,[38] this means that concentration fluctuations with all values of k will grow initially, and there will be no common point of intersection of the curves. When higher-order terms are included in the expansion of $f(x)$, the above inequality will cease to be valid for large k and a common point of intersection may appear.[97] The results reported by Neilson,[93] who observed a common point of intersection in the case of scattering curves recorded for slowly quenched specimens of SiO_2–12.6 mol.% Na_2O, appear to refer to the nonlinear stages of decomposition. Moreover, Srinivasan *et al.*[97] detected local peaks on the $I(k)$ curves during the nonlinear decomposition stages, which corresponded to higher harmonics of the fundamental spinodal wavelength.

Simmons *et al.*[100] investigated phase separation in the Na_2O–B_2O_3–SiO_2 system of critical composition by the viscosity method. They found a substantial reduction in viscosity during cooling of the glass from a temperature substantially exceeding T_c down to temperatures just below T_c. They used these data to conclude that phase separation in this system occurred via the nucleation and growth mechanism. They explained this result by supposing that nucleation was kinetically more favored than spinodal decomposition even below the spinodal curve if the temperature was close to T_c. This conclusion was reached by assuming that the size of the fluctuations necessary to produce a critical nucleus was less than λ_c. However, since both quantities, i.e., the minimum size of the nucleus and the critical wavelength of instability are of the order of the correlation length near T_c, there is considerable doubt as to the validity of this interpretation.

Diffraction data suggest that the spinodal mechanism operates in glasses during phase separation in the region of unstable states. There are, however, considerable discrepancies between the predictions of the linearized Cahn theory and experimental results. The agreement between theory and experiment can be improved by taking thermal fluctuations in composition into account.[38,97] On the other hand, a more detailed comparison between experimental data and the theory of the early stages of spinodal decomposition will require sufficiently homogeneous quenched specimens to begin with, i.e., the quenching time must not exceed the phase separation time. It is not always certain whether this is so, although acceptable initial conditions have been achieved in many cases. For example, Zarzycki[99] used an analysis of the Ornstein–Zernike graphs (I^{-1} plotted against k^2) for $T>T_c$ and $T<T_c$ to conclude that the spectrum of fluctuations in a rapidly quenched specimen corresponded to the fluctuation spectrum above T_c, i.e., the quenching conditions were satisfactory.

C. Binary liquid mixtures

Studies of spinodal decomposition in binary liquid mixtures encounter considerable difficulties because the characteristic decomposition times are short, due to the high (in comparison with solids) diffusion coefficients. It would appear that spinodal decomposition can be observed in nonviscous liquid mixtures only near the critical point since, firstly, diffusion is markedly slowed down in the critical region and, secondly, it is possible to take the system from the stable to the labile region through the critical point without going through the metastable region (Fig. 2).

Spinodal decomposition in liquids was first observed by Huang *et al.*[101] They used monochromatic-light scattering to investigate phase separation in the methanol-cyclohexane system near the critical point. The depth of penetration into the labile region was 2×10^{-3} °K with the system thermostated to better than 0.4×10^{-3} °K over a period of 15 minutes. The angular distribution of the scattered light intensity was recorded by photomultipliers and on photographic film. When the system was taken into the region of unstable states, a ring corresponding to maximum scattered intensity appeared on the photographic plate mounted at right-angles to the incident beam. The radius of the ring corresponded to a scattering angle of 0.05 rad or a scattered wave vector $k_m\approx7\times10^4$ cm^{-1}. The appearance of the ring indicated that a characteristic size $\lambda_m=2\pi/k_m$ had evolved in the system. The diameter of the ring remained constant over a period of the order of a few minutes. It then decreased and the ring eventually disappeared. The time of existence of the ring decreased with increasing depth of penetration into the labile region. The wave vector k_m corresponding to maximum scatter-

ing amplitude was in good agreement with the wave vector corresponding to maximum growth as estimated from Cahn's theory. Over a period of about one minute after the temperature was reduced, the scattered intensity increased exponentially with constant k. The graph of R/k^2 against k^2 was nearly linear for small values of k, but very nonlinear elsewhere. We thus have clear evidence for spinodal decomposition during the early stages.[101] However, it has been noted[104] that these results must be treated with caution from the quantitative point of view because the specimen cell used in the experiments[101] was relatively thick (~1 cm), so that there should have been a considerable contribution due to multiple scattering and the time necessary to establish thermal equilibrium was quite long.

An analogous experimental technique has been used to investigate spinodal-decomposition kinetics in the 2, 6-lutidine-water system with a lower critical point.[102-104] Special attention was paid to the nonlinear stages of spinodal decomposition, which are characterized by a time dependence of k_m, and the integrated intensity of scattered light. The experimental data were not in agreement[105] with Langer's theory in the mean-field approximation.[41] The phase-separation kinetics in the spinodal region was found to be very dependent on the superheating $T-T_c$. For $T-T_c<2\times10^{-3}$ °K, the dependence of k_m and $I(k_m)$ on t was in good agreement with the Kawasaki theory.[47] However, for $T-T_c\gtrsim2\times10^{-3}$ °K, there was no such agreement, and this may have been connected with the finite rate of variation of temperature in the experiment. Microphotography[103] was used to investigate the late stages of phase separation (1 min $\lesssim t\lesssim$ 1.5 h). The growth in the mean size of droplets was approximated by $l\sim t^{1/3}$ for all the values of $T-T_c$ under investigation.

Wong and Knobler[106] have used an interesting technique for taking a binary liquid system into the region of unstable states. This method is based on the fact that the critical temperature is a function of pressure. A critical mixture of isobutyric acid and water, for which $dT_c/dp=-0.055$ °K·atm^{-1} was taken into the labile region by rapidly varying the applied pressure at constant temperature. The depth of penetration into the labile region was between 10^{-3} and 9.2×10^{-3} °K. The angular and time dependence of the scattered monochromatic radiation was investigated. In contrast to previous work,[101] $I(k)$ did not grow exponentially even in the early stages of decomposition. Wong and Knobler[106] do not reproduce the experimental curves for $I(k,t)$ and discuss only the dependence on time and depth of penetration into the labile region for $\tilde{I}(\tilde{k}_m)$ and $\tilde{k}_m$. In accordance with Langer's theory in the scaling form,[42] they found that the dependence of the scaled quantities $I(k_m)$ and k_m on the scaled time $\tilde{t}$ had a universal form independent of T_c-T. The data of Wong and Knobler appear to be more reliable from the point of view of comparison with theory because their experimental technique[106] ensures a very rapid transition of the system into the labile region, and avoids difficulties connected with the finite time necessary to establish thermal equilibrium.

Observations of spinodal decomposition in polymer solutions have also been reported.[107-111] Solutions of high-molecular-weight liquids are distinguished by high viscosity and low diffusion coefficients as compared with low molecular solutions. The characteristic decomposition time of high-molecular solutions is therefore greater than that of low-molecular solutions, and greater penetration into the region of unstable states becomes possible.

D. Computer simulations

An interesting new direction in the study of spinodal decomposition kinetics is computer simulation using the Monte Carlo and molecular dynamics methods. This simulation is based on an assumed interaction potential between the atoms and on the rules for the interchange of atoms in the lattice. The results of such simulation experiments do not, of course, depend on the phenomenological theory. Thus, Bortz[112] has discussed a simple one-dimensional model of a binary alloy consisting of 200 atoms (100 atoms of type A and 100 of type B) with periodic boundary conditions. Each site in the linear chain was assigned $X_i=+1$ or $X_i=-1$, depending on whether it was occupied by an atom A or atom B. The interaction energy was taken in the form

$$E=-J\sum_{0<|i-j|\leq n}X_iX_j, \tag{5.1}$$

where J is a positive constant and n is the interaction interval. Since a short-range potential does not yield a phase transition at a finite temperature in a one-dimensional system, the interaction potential is chosen to be of the long-range type ($n=15$). The evolution of the system from a random initial configuration is specified as follows. A pair of neighboring sites is chosen randomly. If these sites are occupied by different atoms, the possibility of permutation is considered. The energy difference ΔE between the existing configuration and the configuration after a given permutation is computed. If the exchange probability

$$P=\frac{\exp(-\Delta E/k_BT)}{1+\exp(-\Delta E/k_BT)}$$

exceeds some random number $R\leq1$, the two atoms are interchanged. Repeated application of this procedure simulates diffusion in the binary alloy. The local concentration at the site i is defined as the average over the set $\{X_j\}$, $i-n\leq j\leq i+n$, i.e., over all the sites with which site i interacts. This definition of local concentration satisfies the condition that the concentration must vary slowly between successive lattice sites and, if the parameters are suitably chosen, it can be compared with the numerical solution of the generalized diffusion equation given by (3.4).

One of the simulation experiments[112] is illustrated in Fig. 10. As can be seen, there is a clear periodic structure at the intermediate decomposition stage (Fig. 10b), which becomes coarser during the later stages (Fig. 10c). The segregation of two spatially separated phases is observed for all initial configurations. A comparison was also carried out with the phenomenological theory. The evolution of the system described by the generalized diffusion equation during the early

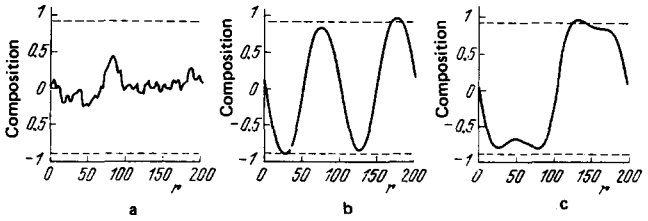

FIG. 10. Evolution of concentration profiles in a one-dimensional model system in the region of unstable states.[112] The distance r along the chain is measured in units of the lattice constant. $T/T_c = 0.615$. a) $t = 200$; b) $t = 1.07 \times 10^6$; c) $t = 7.32 \times 10^6$ (time in arbitrary units). Dashed lines show equilibrium phase compositions.

stages of decomposition is in good agreement with simulations of the diffusion process. However, it has been shown[112] that, for certain initial configurations, the generalized diffusion equation does not describe the coarsening of the structure during the later decomposition stages: the system remains in the metastable state (represented by Fig. 10b) for an infinite time. The reason for this is that thermal concentration fluctuations were not taken into account in Cahn's theory. Monte Carlo simulations are thus seen to confirm the limited validity of the generalized diffusion equation given by (3.4), in accordance with Langer's analysis.[41]

An analogous technique has also been used to simulate spinodal decomposition in two-dimensional[113,114] and three-dimensional[115,116] systems. Only nearest-neighbor interactions were taken into account [$n = 1$ in (5.1)]. Bortz *et al.*[114,116] investigated mainly the behavior of the structure factor $S(\mathbf{k}, t)$. The temporal evolution of this factor, averaged over a spherical layer in reciprocal space, is shown in Fig. 11. The peak on the $S(\mathbf{k}, t)$ curve is seen to grow and shift toward smaller k. Simulation results[115] are in qualitative agreement with numerical results deduced from Langer's theory.[42] Bortz *et al.*[116] have also investigated the cluster size distribution and the cluster growth kinetics during the decomposition process.

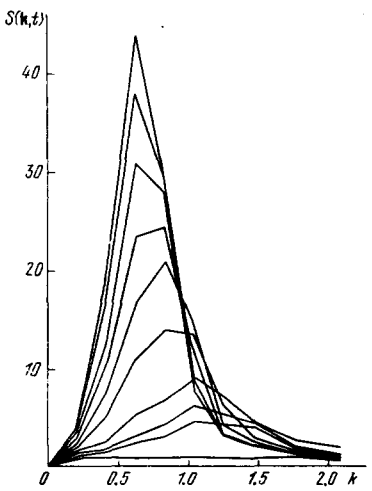

FIG. 11. Evolution of the structure factor $S(\mathbf{k}, T)$ in a three-dimensional model system at $T = 0.59T_c$.[115] The times (increasing upward) are: 0, 16.7, 28.0, 54.1, 129.7, 215.2, 308.2, 405.7, 507.6, 613.0 (S, $\mathbf{k}$, t in arbitrary units).

An interesting computer "experiment" has been carried out by Abraham *et al.*[117] They simulated spinodal decomposition in a one-component system by the molecular dynamics method. They carried out a numerical solution of the classical equations of motion for a system of 1372 atoms interacting via the Lennard-Jones potential, using periodic boundary conditions. As already noted, spinodal decomposition in a one-component liquid is difficult to observe because the characteristic decomposition times are very short. Abraham *et al.*[117] estimate that this time is of the order of 5×10^{-11} sec. Mathematical simulation can be used to perform an instantaneous transformation of the system to the unstable state, and offers a unique way of observing the early decomposition stages at the molecular level. In accordance with the predictions of Cahn's theory,[33] there was a continuous growth in density fluctuations and a coherence structure consisting of regions with high and low densities appeared in the early stages of decomposition.

6. APPROXIMATE SPINODAL CURVES

The description of nonequilibrium phase transitions has encountered considerable difficulties. This is quite clear in the case of spinodal decomposition. The very definition of a spinodal curve is introduced on the basis of an extension of the range of validity of thermodynamics that is not fully justified.

Instability conditions of the form $(\partial p/\partial \rho)_T < 0$, $(\partial \mu_1/\partial x_1)_T < 0$ are acceptable only if they can be used to exhibit regions of actual instability of aggregated and phase states of a given system. This presupposes the existence of single-valued continuous and differentiable functions (free energy, the equation of state) beyond the limit of absolute phase stability, i.e., in the interior of the binodal curve of Fig. 1, 2 and the segment $AabB$ in Fig. 12. Moreover, the subcritical van der Waals isothermals with a minimum and a maximum are neither the result of a rigorous theory nor verified experimentally. They are predicted by the mean-field theory and certain other approximate models.

A degree of justification for the van der Waals loop is provided by the following. The existence of supersaturated (metastable) states has been established experimentally. For example, the liquid and gas branches of the isothermal cut the phase equilibrium line (AcB in Fig. 12) in opposite directions and penetrate quite deeply into the region of incomplete stability. The initial segments of the "loop" can thus be located quite definitely. They are indicated by AA' and BB' in Fig. 12.

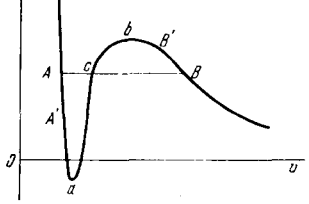

FIG. 12. Subcritical van der Waals isotherm for a liquid-vapor system. AcB is the equilibrium transformation line.

The metastable state corresponds to a local minimum of the thermodynamic potential (for example, the free energy). The height of the barrier that must be overcome by the system in the course of spontaneous transition to an absolutely stable state for given external conditions is determined by the work W_* that must be performed to produce the critical nucleus of the competing phase. However, the free energy of the system has not one but a large number of local minima of different depth if we represent the hypersurface F as a functional of the spatial distribution of the molecules. To remove the ambiguity in the description of stable states, we must use a system in which the relaxation time τ_i are much shorter than the mean nucleus expectation time $\langle\tau\rangle$. The metastable state can then be associated with definite values of thermodynamic parameters that are independent of the prehistory of the system. The quasistatic condition in the metastable region can be written in the form

$$\left\{\tau_i = \frac{l}{v_i}\right\} \ll \mathcal{T} < \langle\tau\rangle,$$

where l is a typical linear dimension of the system, v_i is the rate of approach to equilibrium in the i-th parameter, and $\mathcal{T}$ is the characteristic time of the experiment.

As can be seen, the thermodynamic description of metastable states presupposes more complete information about the system (knowledge of $\langle\tau\rangle$) than is required for a completely stable state. Nonequilibrium states can be described in thermodynamics with the aid of a "gedanken experiment."[118,119 4)]

The simplest and most convenient object for investigating metastable states and the limits of stability is the superheated one-component liquid. Active boiling centers can easily be avoided by using small glass ampules. The low viscosity of the superheated liquid guarantees rapid relaxation of its structure which is not always the case for supercooled liquids. Surface tension on the liquid-vapor boundary can be measured directly at different temperatures. These data are essential if the spinodal curve of a superheated liquid is to be approximated by the Furth hole theory[120] and the theory of homogeneous nucleation verified. Mean expectation times $\langle\tau\rangle$ of the order of minutes or seconds have been observed at temperatures and pressures that are in good agreement with theoretical predictions.[121] Figure 13 shows the saturation line for argon,[122] the theoretical spontaneous-boiling boundary for nucleation frequency $J \approx 100$ cm$^{-3}\cdot$sec^{-1}, the experimental points corresponding to this value of J, and the spinodal curve.

Direct measurement of the specific volume,[122-125] ultrasound velocity,[126,127] viscosity,[128,129] and thermal conductivity[130] of liquids with deep penetration into the region of superheated states have been carried out. All these parameters cross the binodal curve without singularity. Experimental data indicate that metastable states do not segregate during a gradual change of phase.

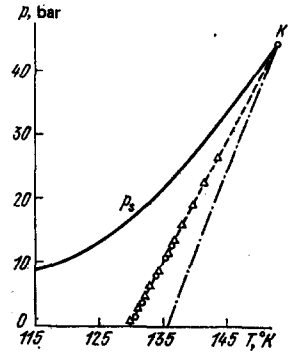

FIG. 13. Equilibrium vapor-pressure curve $p_s(T)$ and spontaneous boiling boundary for superheated liquid argon. Points—experimental, dashed curve—calculated from the theory of homogeneous nucleation, dot-dash curve—spinodal.

Figure 14 shows a series of isothermals for diethyl ether[131] in the form of specific volume plotted against pressure. Figure 15 shows the measured velocity of sound in liquid xenon.[126] Segments of the isothermals to the left of the line u_s refer to the superheated liquid. The example of water was used to show[124] that the change in specific volume during superheating could be accurately described by the international equation of state constructed with great care for the stable region.

Existing data thus support the conclusion that the superheated liquid (under controlled experimental conditions) is in an internal state of equilibrium. The equilibrium is incomplete only in relation to the formation of a new phase (vapor) with known free-energy barrier $W_* = W_*(p, T)$. This is a necessary prerequisite for an unambiguous thermodynamic description of superheated liquids.

The spinodal curve can be determined from the condition $(\partial p/\partial v)_T = 0$ using the equation of state approximating experimental data in the stable and metastable regions. In addition to Fig. 13, the spinodal curve for liquid argon is shown in terms of reduced thermodynamic coordinates in Figs. 16 and 17 together with the results of calculations based on different models and approximations.[132-134]

When plotted on the p, T plane, the spinodal curve of a

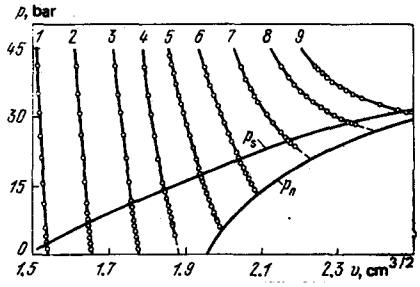

FIG. 14. Isotherms for diethyl ether with penetration of the region of metastable (superheated) states of the liquid: 1–9 corresponds to the temperature interval 71.1–186.7 °C, p_s—saturation line, p_v—spontaneous boiling line ($J \approx 10^2$ cm$^{-3}\cdot$sec^{-1}).

4)We note that "gedanken" experiments requiring the introduction of restrictions that are difficult to implement can be performed by using, for example, the Monte Carlo method in a computer simulation.

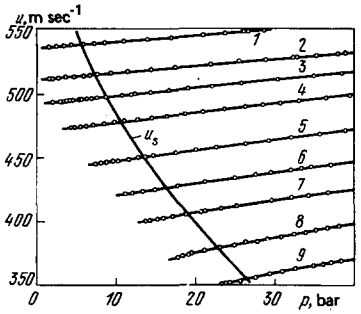

FIG. 15. Velocity of ultrasound plotted against pressure ($1-T=202.1$ °K, ..., $9-T=253.5$ °K) in stable and superheated (to the left of the u_s line) liquid xenon.

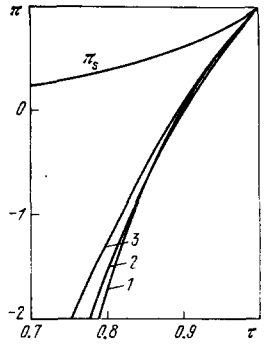

FIG. 16. Spinodal curve for superheated liquid argon in reduced coordinates: temperature $\tau=T/T_c$, pressure $\pi=p/p_c$: 1—equation of state,[125] 2—Furth theory,[120] 3—Ref. 132, π_s—equilibrium vapor pressure.

one-component system is the envelope of a family of isochores.[121] This property can be used to obtain an approximation to the spinodal curve. This has been found useful in the qualitative discussion of stability. For example, it was found, unexpectedly, that the $v(p,T)=\text{const}$ isochores near the melting line were such that their continuation into the supercooled region could not be used to construct an envelope. Analysis of this situation has led[135] to the conclusion that a supercooled one-component liquid does not have a spinodal curve.[5)] Each of the aggregated states has only one essential long-wave instability boundary $(\partial p/\partial\rho)_T=0$ (vapor on the side of supersaturation, liquid and crystal on the side of superheating or tension).

For two-component stratifying solutions, the spinodal is determined from the condition $(\partial\mu_1/\partial x_1)_{T,p}=0$ by extrapolating experimental data from the stable to the metastable region. The partial vapor pressure p_i above the solution or the scattered light intensity I can be taken as the initial quantity. For given concentration of solution and angle and aperture of scattering, we have $I^{-1}\sim(\partial\mu_1/\partial x_1)$. [In the approximation of linear thermodynamics of irreversible processes, there is also a proportionality between I^{-1} and the diffusion coefficient D; see (2.10).] The reciprocal of the scattered intensity is an almost linear function of temperature. Extrapolation of this graph can be used to determine the temperature at points on the spinodal for the corresponding concentrations.[6)] Figure 2 shows the spinodal for the isobutyric acid-water system and Fig. 18 shows the binodal and spinodal of a further system constructed on the basis of data reported in Ref. 137.

The spinodal of a solid solution is difficult to approximate because the influence of internal elastic stresses is difficult to control. In addition, there may be other unrelaxed parameters. Figure 19 shows the suggested shift of the spinodal of the Au–Ni solid solution due to elastic stresses.[138]

The spinodal corresponds to the long-wave instability boundary. This justifies the use of macroscopic compressibility, specific heat, or the derivative $\partial\mu_1/\partial x_1$ in obtaining the approximate spinodal. It would be interesting to establish the connection between the short-wave and long-wave instabilities. If we take the approximation given by (3.1) for the free energy, the onset of short-wave instability will always indicate the existence of long-wave instability as well ($k\to 0$). However, we cannot be sure about the generality of this result. The relationship between static (thermodynamic) and dynamic (soft-mode) instability criteria is also important. The pseudoharmonic approximation has been used by Zyryanov *et al.* to investigate the stability of a crystal lattice. They conclude that thermodynamic stability criteria are quite general. For the example of a linear chain, they[139] show that the onset of dynamic instability in the ground state is accompanied by a violation of the conditions of thermodynamic stability.

The spinodal problem is, in many ways, analogous to problems concerned with the determination of stability boundaries in mechanics, e.g., in the theory of oscillations. The fact that, in a sense, states (motions) in the instability region are unobservable is no bar to the determination of the boundary of this region. On the stability boundary, the system is not usually described by the equations from which this boundary has been determined. However, the behavior of the system in the stable region contains sufficient information to enable us to determine the stability boundary to a good precision. This situation is characteristic not only for mechanical but also for thermodynamic systems.

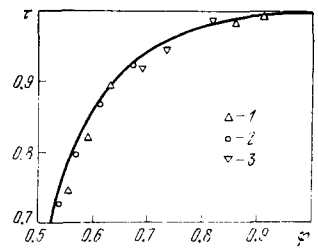

FIG. 17. Projection of the spinodal curve of argon onto the temperature-specific volume plane, $\varphi=v/v_c$: solid line—equation of state,[125] 1—hole theory,[132] 2—hyperchain theory,[133] 3—Percus-Yevick theory.[134]

[5)]This phenomenon is in agreement with the well-known proposition[136] that there is no critical point in the crystal-melt equilibrium, and reflects the qualitative difference between regular and irregular (amorphous) structures.

[6)]The stability boundary obtained in this way is sometimes referred to as the pseudospinodal because linear extrapolation into the region of metastable states is not very reliable.

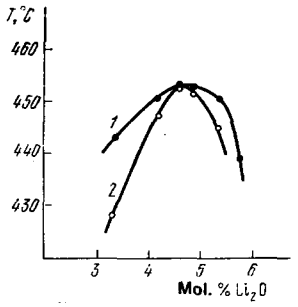

FIG. 18. Phase diagram for the B_2O_3-Li_2O system:[137] 1—binodal, 2—spinodal.

Studies of critical phenomena have led to the concept of nonanalyticity of the free energy at the critical point. The question is whether the critical point is the only singularity on the thermodynamic surface of states or whether this is a property of the entire spinodal. This question was put forward and discussed in Refs. 121, 140, 141, and 142. It is important to note that, with increasing distance from the critical point, the region in which the singularity has an appreciable influence on the behavior of the medium should contract if the singularity generally persists on the spinodal. Studies of metastable states have so far yielded no indication that the approximation of the spinodal based on the "classical" thermodynamic potential should be abandoned.

7. NUCLEATION AND SPINODAL DECOMPOSITION

Small fluctuations are resorbed in the metastable region, but they are amplified by the reaction of the system in the unstable region. In both cases, the response of the system to a perturbation of a homogeneous state corresponds to a reduction in the thermodynamic potential under given external conditions. Spinodal decomposition may be regarded as a nonactivated process. Conversely, a spontaneous phase transition from the metastable state requires activation. The appearance of a persistent nucleus in the system is the result of a sufficiently large (and generally rare) fluctuation.

This can be seen from the following. According to the theory of homogeneous nucleation,[9-12,121] the stationary nucleation frequency $J = 10\ \text{cm}^{-3} \cdot \text{sec}^{-1}$ in a superheated liquid corresponds to $W_* = \Delta F$ (the work done in producing the critical nucleus) of the order of $70 k_B T$. Such fluctuations can be observed in the course of a normal experiment only in a relatively large system.

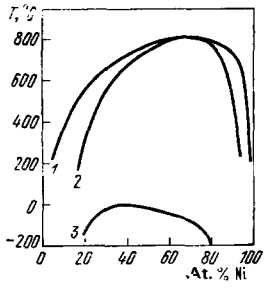

FIG. 19. Binodal (1), "chemical" spinodal (2), and "coherent" spinodal (3) of the Au-Ni system according to the data from[138].

On the saturation line, we have $(W_*/k_B T) \to \infty$. The barrier height $G = W_*/k_B T$ decreases with penetration into the metastable region. For a spherical nucleus in vapor, we have[11,121]

$$W_* = \frac{16\pi\sigma^3}{3(p_S - p')^2[1-(v'/v'')]^2}; \qquad (7.1)$$

where σ is the surface tension on the liquid-vapor boundary, p_S is the pressure on the equilibrium line (binodal), p' is the pressure in the metastable liquid, and v', v'' are the specific volumes of the liquid and vapor on the binodal. All the quantities in (7.1) are taken as the usual macroscopic parameters. This assumption seems inappropriate *a priori* for the description of a microheterogeneous system in which the dispersed phase contains 100–1000 molecules.

However, systematic studies of nucleation kinetics in superheated liquids under different pressures, using different techniques[121,122,143,144] have revealed satisfactory agreement between theoretical predictions[9-12] [see (2.1) and (7.1)] and experiment. This agreement prevails over a broad range of nucleation frequencies, as can be seen from Fig. 20. The surface tension σ can be estimated from the measured nucleation frequency J and certain other directly measured parameters by inverting (2.7) and (7.1). As a rule, the values of surface tension estimated in this way differ from the "macroscopic" values by 1–3%, which is within experimental uncertainty.

It is appropriate at this point to consider an example illustrating the variation of $G, J, \langle\tau\rangle$ with the degree of superheating of the liquid. Let us take diethyl ether at atmospheric pressure. The saturation temperature T_S is 34.5 °C. The values $G_1 = 100$ and $G_2 = 40$ correspond to liquid temperature $T_1 = 140$ °C and $T_2 = 148$ °C, respectively. These temperatures refer to highly superheated states of the liquid. The degree of stability of the metastable phase will be judged by considering the spontaneous nucleation frequency per unit volume J or the mean expectation time per unit volume $\langle\tau\rangle = 1/J$. If we use this approach, we find an enormous difference in stability (phase transition kinetics) in these two cases. According to the Volmer–Döring–Zel'dovich–Frenkel

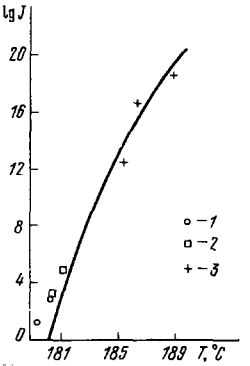

FIG. 20. Temperature dependence of nucleation frequency J ($\text{cm}^{-3} \cdot \text{sec}^{-1}$) in *n*-hexane at atmospheric pressure: solid line—theoretical, points—experimental,[121] 1—experiments with miniature bubble chamber; 2—superheated drops; 3—pulsed heating.

theory, we have

$$J_1 \approx 10^{-11}\ \text{cm}^{-3}\ \text{sec}^{-1}, \quad \langle\tau\rangle \approx 10^{11}\ \text{sec} \approx 3\cdot 10^{3}\ \text{yr},$$
$$J_2 \approx 10^{15}\ \text{cm}^{-3}\ \text{sec}^{-1}, \quad \langle\tau\rangle \approx 10^{-15}\ \text{sec}.$$

The theoretically predicted increase in J by 26 orders of magnitude corresponds to a temperature change of only 8° when the superheating $T - T_S$ exceeds 105°. We have already noted the good agreement between theory and experiment. For example, when $p = 1$ bar, the value $J = 100\ \text{cm}^{-3}\cdot\text{sec}^{-1}$ is predicted to occur at 143.6 °C, whereas experiment[121] yields 143.2 °C. The experimental and theoretical values of the quantity $(d\ln J/dT) \approx -(dG/dT)$ are also close to one another. The radius of the critical bubble and the number of molecules contained in it are estimated to be $r_* \approx 5.3\times 10^{-7}$ cm, $n_* \approx 250$.

This example was intended to indicate the existence of a quite sharp (in supersaturation) boundary of spontaneous phase transition of the first kind and the validity of the predictions of the kinetic theory of nucleation.

The energy characteristic of a nucleus (7.1) can be supplemented by estimates of the density (concentration) gradient in the surface layer. If we denote the layer thickness by δ and the density (concentration) difference between the coexisting phases by $\Delta\rho(\Delta x)$, we obtain

$$|\nabla\rho| \approx \frac{\Delta\rho}{\delta}, \qquad |\nabla x| \approx \frac{\Delta x}{\delta}.$$

We assume that supersaturation is quite large, for example, $G \lesssim 70$. Since, in general, the surface layer occupies only part of the volume of the nucleus, $\delta < r_*$, we have

$$|\nabla\rho| > \frac{\Delta\rho}{r_*}, \qquad |\nabla x| > \frac{\Delta x}{r_*}. \tag{7.2}$$

The production of a nucleus by the fluctuation mechanism is accompanied by the appearance of a radial density (concentration) gradient in a region of linear size of the order of r_*, satisfying (7.2). In the metastable state, only a small fraction of local fluctuations will satisfy this condition. Most of them will be reversibly resolved. The nuclei cannot appear in unstable states until the growth of the fluctuation produces a stable surface layer. Individual small portions of the system are in the metastable region during this process.

The problem of determining the boundary of essential instability in terms of nucleation concepts was considered by Gibbs.[4] Violation of the condition $(\partial p/\partial\rho)_T > 0$ prevents the appearance of the stable layer separating the two phases. (One of the phases is assumed to be dispersed and it is only then that one can ensure equilibrium between the metastable and stable phases. This equilibrium is unstable.) Gibbs noted that the spinodal should be close to the boundary on which surface tension vanishes. However, if at any temperature $\sigma \to 0$ as the spinodal is approached, the barrier height W_* will tend to zero during the nucleation process, and the nucleation frequency will tend to the maximum value of about $10^{29}\ \text{cm}^{-3}\cdot\text{sec}^{-1}$. The separation into heterophase and homophase fluctuations becomes meaningless when $W_* \lesssim k_B T$. The mechanism responsible for the phase transition is modified near the spinodal so that spinodal decomposition and nucleation form the beginning and end of a complex continuous process involved in instability development. As shown above, the diffusion coefficient and the amplification factor change sign on the spinodal in the long-wave limit.

The parameters r_* and $\langle\tau\rangle$ may be looked upon as the characteristic length and time of instability development in the case of nucleation during a spontaneous phase transition from a metastable state. The radius of the critical nucleus decreases with increasing degree of supersaturation. The minimum value of r_* is of the order of the correlation length l_c. The parameters r_* and $\langle\tau\rangle$ are analogous to λ_m, R_m^{-1} in the case of spinodal decomposition. This analogy becomes clearer if we recall that the minimum instability wavelength λ_m is also of the order of l_d. The time $\langle\tau\rangle$ is determined by diffusion in the space of $f(n) - n$, where $f(n)$ is the size distribution function of the nuclei of the new phase and R_m^{-1} is determined by diffusion in ordinary space.

The basic irreversibility of the phase transition is connected with nucleation and spinodal decomposition. The reverse transition of a macroscopic two-phase system to the single-phase state in the case of a quasistatic variation in external parameters will occur along the line of phase equilibrium without entering the region of metastable states.

8. COMPARISON OF THEORY WITH EXPERIMENT

Cahn's theory rests on the basic ideas of Landau's theory of the self-consistent field.[136] As we approach the spinodal, we can enter a region of strong interaction between fluctuations, where the representation of free energy by (3.1) may no longer be valid. It is well known that the condition for the validity of the self-consistent field theory is that the fluctuations are weak, and this can be expressed in the form of Ginzburg's criterion[145]

$$\text{Gi} \ll |\varepsilon|, \tag{8.1}$$

where $\varepsilon = (T - T_c)/T_c$ and Gi is constructed from the expansion coefficients of the free energy. It has been estimated[146] that, in order of magnitude,

$$\text{Gi} = \left(\frac{r_0}{l_0}\right)^6,$$

where l_0 is the correlation length well away from the spinodal and r_0 is the range of interaction in the system. For binary liquid mixtures and liquid-vapor systems, $\text{Gi} \approx 0.01$–0.001. The experiments reported in Refs. 101–106 were performed for $|\varepsilon| < 10^{-4}$. Cahn's theory and its modifications based on the idea of the self-consistent field are therefore hardly valid in this context. Experiments with alloys and glasses are usually performed with supercoolings $|\varepsilon| \approx 0.1$–$1$, so that condition (8.1) may be approximately satisfied.

Patashinskiĭ and Yakub[147] proposed the following criterion for the validity of the linearized theory near T_c:

$$\frac{\text{Gi}}{\varepsilon_0 \tilde{D}^4} \ll 1, \tag{8.2}$$

where ε_0 is the reduced temperature of the initial (stable) state and D is the dimensionless diffusion coefficient[49] which vanishes on the spinodal. It is assumed that the system undergoes an instantaneous transition from the initially stable to the unstable state. Near the

spinodal, where $|\tilde{D}| \ll 1$, (8.2) is more difficult to satisfy than (8.1) and one would expect that relaxation is always nonlinear in this region. This conclusion refers, above all, to experiments with binary liquid mixtures in the neighborhood of the critical point. Manifestations of nonlinearity during the early stages of spinodal decomposition in the case of experiments with highly supercooled alloys and glasses are probably connected not with (8.2), but with the finite rate of cooling.

When a linear stage of decomposition is known to occur, the time of validity of the linear Cahn theory, t_l, can be estimated from[147]

$$t_l \sim \frac{\ln (\mathrm{Gi}/\varepsilon_0)}{2R(k_m)}.$$

When (3.7) is valid, the amplitudes $A(k)$ in the wave vector interval

$$\Delta k \sim \frac{k_m}{\sqrt[4]{\ln (\mathrm{Gi}/\varepsilon_0)}}$$

remain of the same order of magnitude over the time t_l. For the systems discussed in this review, $|\ln(\mathrm{Gi}/\varepsilon_0)| < 4$ and $\Delta k \sim k_m$. Consequently, we may expect that a structure with well-defined linear size λ_m will not develop by the end of the linear stage and the system will split into "cells" with size variance $\Delta\lambda \sim \lambda_m$.[147] This is supported by the fact that the observed[95] maximum of $R(k)$ is much broader than predicted by Cahn's theory.

The conclusion that the system is unstable under the spinodal for small $k < k_c$ and that it is stable for $k > k_c$ remains valid even beyond the range of validity of Cahn's theory. The overall spinodal decomposition picture should remain qualitatively valid even when the idea of the self-consistent field is abandoned. Since the correlation length predicted by fluctuation theory is more temperature-dependent ($l_c \sim |\varepsilon|^{-2/3}$) than in Landau's theory ($l_c \sim |\varepsilon|^{-1/2}$), it may be expected that k_m will have a stronger temperature dependence than is indicated by the expression $k_m^{-1} \sim l_c$.

The appearance of structure as a result of instability is a relatively general physical phenomenon. In the case of spinodal decomposition, it is due to the growth of fluctuations, in the number of particles and the dispersion of the amplification factor in the absence of directed macroscopic flows of heat, matter, and so on, in the system. Another type of structure appears when such currents are present, but local thermodynamic equilibrium and phase stability are maintained in the system. An example of this is the onset of convection cells in a horizontal layer of a liquid heated from below. Another example is the appearance of spatial periodicity in certain chemical reactions. Such structures have recently attracted considerable theoretical interest.[148,149] The behavior of the system near equilibrium is quite different from its behavior well away from equilibrium. The appearance of structure is connected with the instability of the "thermodynamic" branch adjacent to the region of global equilibrium states. This branch reflects the linear relation between the current and the corresponding generalized force. The formation of cells occurs under conditions of irreversibility and dissipation. The appearance of order is preceded by the growth of fluctuations as a result of instability of the stationary state.

Thus, the onset of structure during spinodal decomposition is not, therefore, an isolated phenomenon without analogies. On the contrary, there is a large class of processes in which ordering proceeds through instability and growth of fluctuations in nonequilibrium thermodynamic systems. Spinodal decomposition is the limiting case of this class when instability appears in the absence of organized flow. Evidently, spinodal decomposition can occur not only in the molecular systems that we have considered but also in magnetic systems. It would be interesting to investigate other cases of spinodal decomposition.

Our review shows that the theory of spinodal decomposition cannot be regarded as complete. Descriptions of the "statics" and dynamics of thermodynamically unstable states have encountered considerable difficulty.[150] Theoretical descriptions of spinodal decomposition reported in the literature are only in qualitative agreement with experiment and, undoubtedly, the theory requires further improvement. Further progress in the theory will require new experimental data on relaxation phase transitions involving thermodynamically unstable states.

The authors are indebted to A. Z. Patashinskiĭ for discussions and useful suggestions.

[1]M. Hillert, Acta Metall. **9**, 525 (1961).
[2]J. W. Cahn, *ibid.*, p. 795.
[3]Ya. B. Zel'dovich and O. M. Todes, Zh. Eksp. Teor. Fiz. **10**, 1441 (1940).
[4]J. W. Gibbs, Papers on Thermodynamics (Russ. transl., Gostekhizdat, M.-L., 1950).
[5]J. W. Gibbs, Elementary Principles of Statistical Mechanics, Yale University Press, 1902 (Russ. Transl., Gostekhizdat, M.-L., 1946).
[6]M. Volmer and A. Weber, Zh. Phys. Chem. **119**, 277 (1925).
[7]L. Farkas, *ibid.* **125**, 236 (1927).
[8]W. Döring, *ibid.* **36**, 371 (1937).
[9]M. Volmer, Kinetik der Phasenbildung, Steinkopf, Dresden, Leipzig, 1939.
[10]Ya. B. Zel'dovich, Zh. Eksp. Teor. Fiz. **12**, 525 (1942).
[11]Ya. I. Frenkel', Kineticheskaya teoriya zhidkosteĭ (Kinetic Theory of Liquids), Nauka, L., 1975.
[12]Yu. Kagan, Zh. Fiz. Khim. **34**, 92 (1960).
[13]I. Prigogine and R. Defay, Chemical Thermodynamics, Longmans, London, 1954 (Russ. Transl., Nauka, Novosibirsk, 1966).
[14]B. Chu, E. J. Schoens, and M. E. Fisher, Phys. Rev. **185**, 219 (1969).
[15]I. R. Krichevskiĭ, N. E. Khazanova, and L. R. Linshits, Inzh.-Fiz. Zh. No. 10, 117 (1960).
[16]V. Daniel and H. Lipson, Proc. R. Soc. London Ser A **181**, 368 (1943).
[17]V. Daniel and H. Lipson, *ibid.* **182**, 378 (1944).
[18]A. J. Ardell and R. B. Nicholson, Acta Metall. **14**, 1295 (1966).
[19]K. J. De Vos, J. Appl. Phys. **37**, 1100 (1966).
[20]Ya. L. Linetskiĭ, E. G. Knizhnik, and B. G. Livshits, Fiz. Met. Metalloved. **29**, 265 (1970).
[21]A. G. Khachaturyan, Teoriya fazovykh prevrashchenii i struktura tverdykh rastvorov (Theory of Phase Transformations and the Structure of Solid Solutions), Nauka, M., 1974.
[22]N. Kraĭdl, in the book: Nauka i chelovechestvo (in: Science and Humanity), Znanie, M., 1973, p. 315.

[23]Yavleniya likvatsii v steklakh (Liquation Phenomena in Glasses), ed. by M. M. Shul'ts, Nauka, L., 1974.
[24]P. F. James, J. Mater. Sci. **10**, 1802 (1975).
[25]P. D. Merica, Trans. AIME **99**, 11 (1932).
[26]R. Becker, Z. Metallkd. **29**, 245 (1937).
[27]U. Dehlinger, *ibid.*, p. 401.
[28]J. W. Cahn, Trans. AIME **242**, 166 (1968).
[29]K. V. Chuistov, in the collection: Metallofizika (Metal Physics), No. 32, Naukova Dumka, 1970, p. 38.
[30]J. W. Cahn and J. E. Hillard, J. Chem. Phys. **31**, 688 (1959).
[31]J. W. Cahn, Acta Metall. **10**, 179 (1962).
[32]J. W. Cahn, *ibid.*, p. 907.
[33]J. W. Cahn, J. Chem. Phys. **42**, 93 (1965).
[34]J. W. Cahn, Acta Metall. **14**, 1685 (1966).
[35]J. E. Morral and J. W. Cahn, *ibid.* **19**, 1037 (1971).
[36]E. L. Huston, J. W. Cahn, and J. E. Hilliard, *ibid.* **14**, 1053 (1966).
[37]K. B. Rundman and J. E. Hilliard, *ibid.* **15**, 1025 (1967).
[38]H. E. Cook, *ibid.* **18**, 297 (1970).
[39]J. S. Langer, Ann. Phys. (N.Y.) **65**, 53 (1971).
[40]J. S. Langer and M. Bar-on, *ibid.* **78**, 421 (1973).
[41]J. S. Langer, Acta Metall. **21**, 1649 (1973).
[42]J. S. Langer, M. Bar-on, and H. D. Miller, Phys. Rev. A **11**, 1417 (1975).
[43]K. G. Wilson, *ibid.* B **4**, 3184 (1971).
[44]D. De Fontaine, Thesis, Northwestern Univ., Evanston, 1967.
[45]Y. Saito, J. Phys. Soc. Jpn. **41**, 1129 (1976).
[46]K. Kawasaki, Prog. Theor. Phys. **57**, 826 (1977).
[47]K. Kawasaki and T. Ohta, *ibid.* **59**, 362 (1978).
[48]T. Ohta and K. Kawasaki, Phys. Lett. A **64**, 404 (1978).
[49]A. Z. Patashinskiĭ and I. S. Yakub, Fiz. Tverd. Tela (Leningrad) **18**, 3630 (1976) [Sov. Phys. Solid State **18**, 2114 (1976)].
[50]A. Z. Patashinskiĭ and I. S. Yakub, Zh. Eksp. Teor. Fiz. **73**, 1954 (1977) [Sov. Phys. JETP **46**, 1025 (1977)].
[51]J. W. Cahn and J. E. Hilliard, J. Chem. Phys. **28**, 258 (1958).
[52]R. W. Hopper and D. R. Uhlmann, Acta Metall. **21**, 35 (1973).
[53]R. W. Hopper and D. R. Uhlmann, *ibid.*, p. 377.
[54]F. F. Abraham, J. Chem. Phys. **63**, 157 (1975).
[55]F. F. Abraham, *ibid.* **64**, 2660 (1976).
[56]J. A. Barker and D. Henderson, *ibid.* **47**, 4714 (1967).
[57]J. D. Weeks, D. Chandler, and H. C. Anderson, *ibid.* **54**, p. 5237 (1971).
[58]F. F. Abraham, *ibid.* **63**, 1316 (1975).
[59]K. Binder, Phys. Rev. B **15**, 4425 (1977).
[60]K. Kawasaki, *ibid.* **145**, 224 (1966).
[61]I. M. Lifshitz, Zh. Eksp. Teor. Fiz. **42**, 1354 (1962) [Sov. Phys. JETP **15**, 939 (1962)].
[62]P. Mirold and K. Binder, Acta Metall. **25**, 1435 (1977).
[63]I. M. Lifshitz and V. V. Slezov, J. Phys. Chem. Solids **19**, 35 (1961).
[64]E. P. Butler and G. Thomas, Acta Metall. **18**, 347 (1970).
[65]D. E. Laughlin and J. W. Cahn, *ibid.* **23**, 329 (1975).
[66]D. E. Laughlin, Acta Metall. **24**, 53 (1976).
[67]R. W. Carpenter, *ibid.* **15**, 1567 (1967).
[68]V. Gerold and W. Merz, Scr. Met. **1**, 33 (1967).
[69]A. Guinier, X-Ray Diffraction, Freeman, N. Y., 1963.
[70]T. L. Bartel and K. B. Rundman, Metall. Trans. A **6**, 1887 (1975).
[71]D. T. Lewandowski and K. B. Rundman, *ibid.* 1895.
[72]S. Agarwal and H. Herman, Scr. Met. **7**, 503 (1973).
[73]M. Murakami, O. Kavano, Y. Murakami, and M. Morinaga, Acta Metall. **17**, 1517 (1969).
[74]A. Naudon, J. Allain, J. Delafond, A. Janqua, and J. Mimault, Scr. Met. **8**, 1105 (1974).
[75]E. Z. Vintaikin and V. Yu. Kolontsov, B sb. Metallovedenie (in: Metallography), Nauka, M., 1971.
[76]J. Vrijen and C. van Dijk, in: Fluctuations, Instabilities and Phase Transitions, ed. by T. Riste, Plenum, New York-London, 1975, p. 43.
[77]C. D. Clark and B. H. Meardon, Nature (London) Phys. Sci. **235**, 18 (1972).
[78]C. D. Clark, S. Messoloras, E. W. J. Mitchell, and R. J. Stewart, J. Appl. Crystallogr. **8**, 127 (1975).
[79]J. Delafond, A. Junqua, J. Mimault, and J. P. Riviere, Acta Metall. **23**, 405 (1975).
[80]A. Junqua, J. Mimault, and J. Delafond, *ibid.* **24**, 779 (1976).
[81]S. Nasu, H. Yasuoka, Y. Nakamura, and Y. Murakami, in: Dig. of Internat. Conference, Kiote-New York, 1972, p. 49.3.
[82]A. C. Yen and T. J. Rowland, Acta Metall. **24**, 409 (1976).
[83]D. Chandra and L. H. Schwartz, Metall. Trans. **2**, 511 (1971).
[84]T. De Nys and P. M. Gielen, *ibid.* 1423.
[85]S. M. Allen and J. W. Cahn, Acta Metall. **24**, 425 (1976).
[86]L. E. Tanner, Philos. Mag. **14**, 111 (1966).
[87]R. Sinclair, J. A. Leake, and B. Ralph, Phys. Status Solidi A **26**, 285 (1973).
[88]H. E. Cook and J. E. Hilliard, J. Appl. Phys. **40**, 2191 (1969).
[89]E. M. Philofsky and J. E. Hilliard, *ibid.* 2198.
[90]J. W. Cahn and R. J. Charles, Phys. Chem. Glasses **6**, 181 (1965).
[91]W. Haller, J. Chem. Phys. **42**, 686 (1965).
[92]T. P. Seward, D. R. Uhlmann, and D. Turnbull, J. Am. Ceram. Soc. **51**, 634 (1968).
[93]G. F. Neilson, Phys. Chem. Glasses **10**, 54 (1969).
[94]M. Tomozawa, R. K. MacCrone, and H. Herman, *ibid.* **11**, 136 (1970).
[95]N. S. Andreev, G. G. Boiko, and N. A. Bokov, J. Non-Cryst. Solids **5**, 41 (1970).
[96]J. Zarzycki and F. Naudin, *ibid.* **1**, 215 (1969).
[97]G. R. Srinivasan, R. Colella, P. B. Macedo, and V. Volterra, Phys. Chem. Glasses **14**, 90 (1973).
[98]A. F. Craievich, Phys. Status Solidi A **28**, 609 (1975).
[99]J. Zarzycki, Discuss. Faraday Soc. **50**, 122 (1970).
[100]J. H. Simmons, P. B. Macedo, A. Napolitano, and W. K. Haller, *ibid.* 155.
[101]J. S. Huang, W. I. Goldburg, and A. W. Bjerkaas, Phys. Rev. Lett. **32**, 921 (1974).
[102]A. J. Schwartz, J. S. Huang, and W. I. Goldburg, J. Chem. Phys. **62**, 1847 (1975).
[103]W. I. Goldburg and J. S. Huang, see Ref. 76, p. 87.
[104]W. I. Goldburg, C. H. Shaw, J. S. Huang, and M. S. Pilant, J. Chem. Phys. **68**, 484 (1978).
[105]A. J. Schwartz, J. S. Huang, and W. I. Goldburg, *ibid.* **63**, 599 (1975).
[106]N. C. Wong and C. M. Knobler, *ibid.* **66**, 4707 (1977).
[107]J. J. Van Aartsen, Europ. Polymer J. **6**, 919 (1970).
[108]J. J. Van Aartsen and C. A. Smolders, *ibid.* 1105.
[109]P. T. Van Emmerik, C. A. Smolders, and W. Geymayer, *ibid.* **9**, 309 (1973).
[110]G. T. Feke and W. Prins. Macromolecules **7**, 527 (1974).
[111]V. M. Andreeva, A. A. Tager, I. S. Tyukova, and L. F. Golenkova, Vysokomol. Soedin. Ser. A **19**, 2604 (1977).
[112]A. B. Bortz, J. Stat. Phys. **11**, 181 (1974).
[113]P. A. Flinn, *ibid.* **10**, 89 (1974).
[114]A. B. Bortz, M. H. Kalos, J. L. Lebowitz, and M. A. Zendejas, Phys. Rev. B **10**, 535 (1974).
[115]J. Marro, A. B. Bortz, M. H. Kalos, and J. L. Lebowitz, *ibid.* **12**, 2000 (1975).
[116]A. Sur, J. L. Lebowitz, J. Marro, and M. H. Kalos, *ibid.* **15**, 3014 (1977).
[117]F. F. Abraham, D. E. Schreiber, M. R. Mruzik, and G. M. Pound, Phys. Rev. Lett. **36**, 261 (1976).
[118]M. A. Leontovich, Vvedenie v termodinamiku (Introduction to Thermodynamics), Gostekhizdat, M.-L., 1952.
[119]H. Reiss, Ber. Bunsenges. Phys. Chem. **79**, 943 (1975).
[120]R. Furth, Proc. Cambr. Philos. Soc. **37**, 252 (1941).
[121]V. P. Skripov, Metastabil'naya zhidkost' (Metastable Liquids), Nauka, M., 1972 (English Transl., Halsted, N. Y., 1974).
[122]V. G. Baĭdakov, V. P. Skripov, and A. M. Kaverin, Zh. Eksp. Teor. Fiz. **65**, 1126 (1973) [Sov. Phys. JETP **38**, 557 (1974)].

[123]G. V. Ermakov and V. P. Skripov, Teplofiz. Vys. Temp. **6**, 89 (1968).
[124]V. N. Chukanov and V. P. Skripov, *ibid.* **9**, 739 (1971).
[125]V. G. Baĭdakov, V. P. Skripov, and A. M. Kaverin, Zh. Eksp. Teor. Fiz. **67**, 676 (1974) [Sov. Phys. JETP **40**, 335 (1975)].
[126]V. G. Baĭdakov and V. P. Skripov, Zh. Fiz. Khim. **50**, 1309 (1976).
[127]G. V. Ermakov and R. G. Ismagilov, Teplofiz. Vys. Temp. **14**, 1097 (1976).
[128]N. V. Bulanov and V. P. Skripov, *ibid.* **12**, 1184 (1974).
[129]N. V. Bulanov and V. P. Skripov, Inzh.-Fiz. Zh. **29**, 1074 (1975).
[130]N. V. Bulanov, E. D. Nikitin, and V. P. Skripov, *ibid.* **26**, 204 (1974).
[131]G. V. Ermakov, V. G. Baĭdakov, and V. P. Skripov, Zh. Fiz. Khim. **48**, 1026 (1973).
[132]M. D. Pena and M. Lombardero, An. Real. Soc. Esp. Fis. y Guin. Ser. A **63**, 7 (1967).
[133]J. De Boer, J. M. J. Van Leeuwen, and J. Groeneveld, Physica **30**, 2265 (1964).
[134]R. O. Watts, J. Chem. Phys. **48**, 50 (1968).
[135]V. P. Skripov and V. G. Baĭdakov, Teplofiz. Vys. Temp. **10**, 1226 (1972).
[136]L. D. Landau and E. M. Lifshitz, Statisticheskaya fizika (Statistical Physics), Gostekhizdat, M.-L., 1951.
[137]V. V. Golubkov, A. P. Titov, T. N. Vasilevskaya, and E. A. Porai-Koshits, Fiz. Khim. Stekla **3**, 306 (1977).
[138]B. Golding and S. C. Moss, Acta Metall. **15**, 1239 (1967).
[139]P. S. Zyryanov, V. V. Kondrat'ev, and I. G. Kuleev, Fiz. Met. Metalloved. **35**, 233 (1973).
[140]A. Compagner, Physica **72**, 115 (1974).
[141]Kh. I. Mogel' and A. V. Chalyĭ, Izv. Vyssh. Uchebn. Zaved. Fiz. No. 12, 146 (1975).
[142]Y. Saito, Prog. Theor. Phys. **59**, 375 (1978).
[143]P. A. Pavlov, E. N. Sinitsyn, and V. P. Skripov, in: Uravneniya sostoyaniya gazov i zhidkostei (Equations of State of Gases and Liquids), Nauka, M., 1975, p. 251.
[144]H. Wakeshima and K. Takata, J. Phys. Soc. Jpn. **13**, 1398 (1958).
[145]V. L. Ginzburg, Fiz. Tverd. Tela (Leningrad) **2**, 2031 (1960) [Sov. Phys. Solid State **2**, 1824 (1961)].
[146]A. Z. Patashinskiĭ and V. L. Pokrovskiĭ, Fluktuatsionnaya teoriya fazovykh perekhodov (Fluctuation Theory of Phase Transitions), Nauka, M., 1975.
[147]I. S. Yakub, Avtoreferat kand. dissertatsii (Abstract of Candidate Thesis), Physicotechnical Institute of Low Temperatures, Academy of Sciences of the Ukrainian SSR, Kharkov, 1979.
[148]P. Glansdorff and I. Prigogine, Thermodynamic Theory of Structure, Stability and Fluctuations, Wiley-Interscience, New York, 1971 (Russ. Transl., Mir, M., 1973).
[149]I. Prigogine and G. Nicolis, Quart. Rev. Biophys. **4**, 107 (1971).
[150]S. J. Langer, Physica **73**, 61 (1974).

Translated by S. Chomet
Edited by M. Hamermesh